PARADIM
AN NSF MATERIALS INNOVATION PLATFORM

LECTURE #3—
NUTS AND BOLTS OF OXIDE MBE: COMPOSITION CONTROL AND CALIBRATION

Darrell G. Schlom

Department of Materials Science and Engineering
Cornell University
Kavli Institute at Cornell for Nanoscale Science
Leibniz-Institut für Kristallzüchtung

Nuts and Bolts of Oxide MBE

AN NSF MATERIALS INNOVATION PLATFORM

How to grow your favorite oxide by MBE?

- ➢ Lecture #2—Growth Conditions, Sources, and Crucibles
- ➢ Lecture #3—Composition Control and Calibration
- ➢ Lecture #4—Epitaxy, Substrates, and Crystal Growth

Composition Control

- **Adsorption-Controlled Growth**
- **Flux-Controlled Growth**

3-Temperature Technique

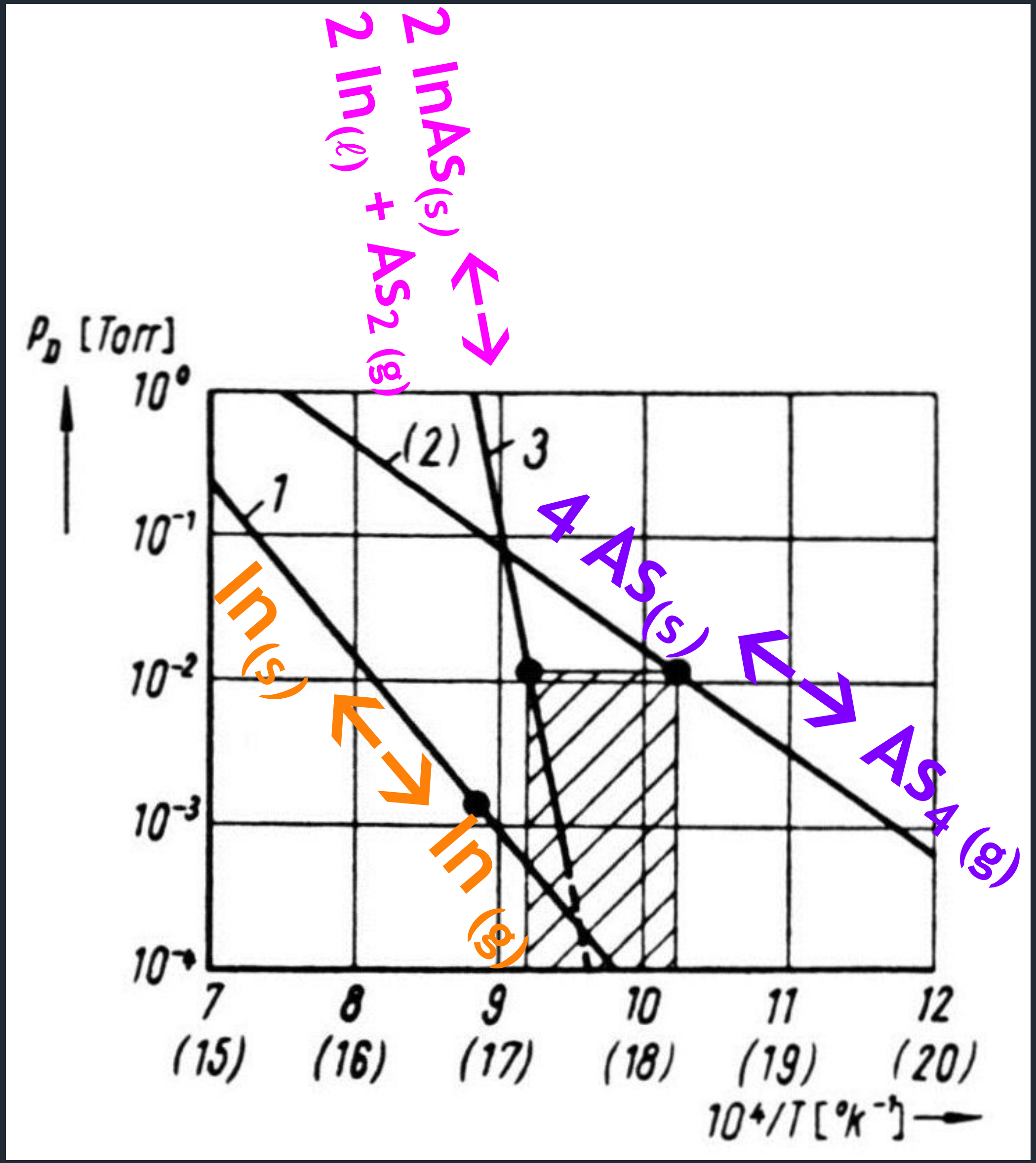

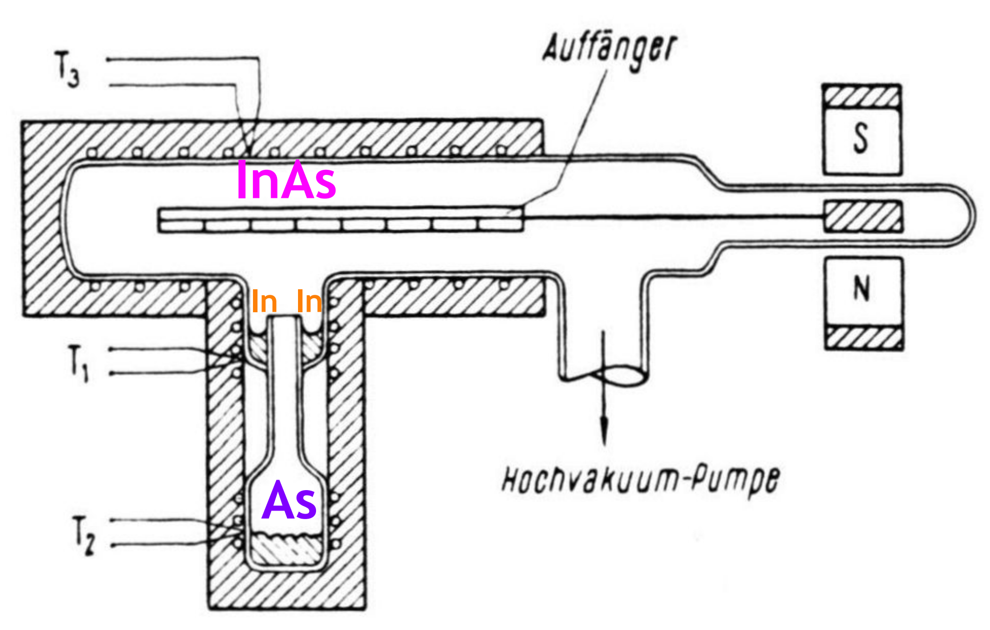

K.G. Günther, “Aufdampfschichten aus halbleitenden III-V Verbindungen,”
Zeitschrift für Naturforschung A **13** (1958) 1081–1089.

A Cold Wall in a Hot-Wall Reactor

CONDICIONES EXTREMAS

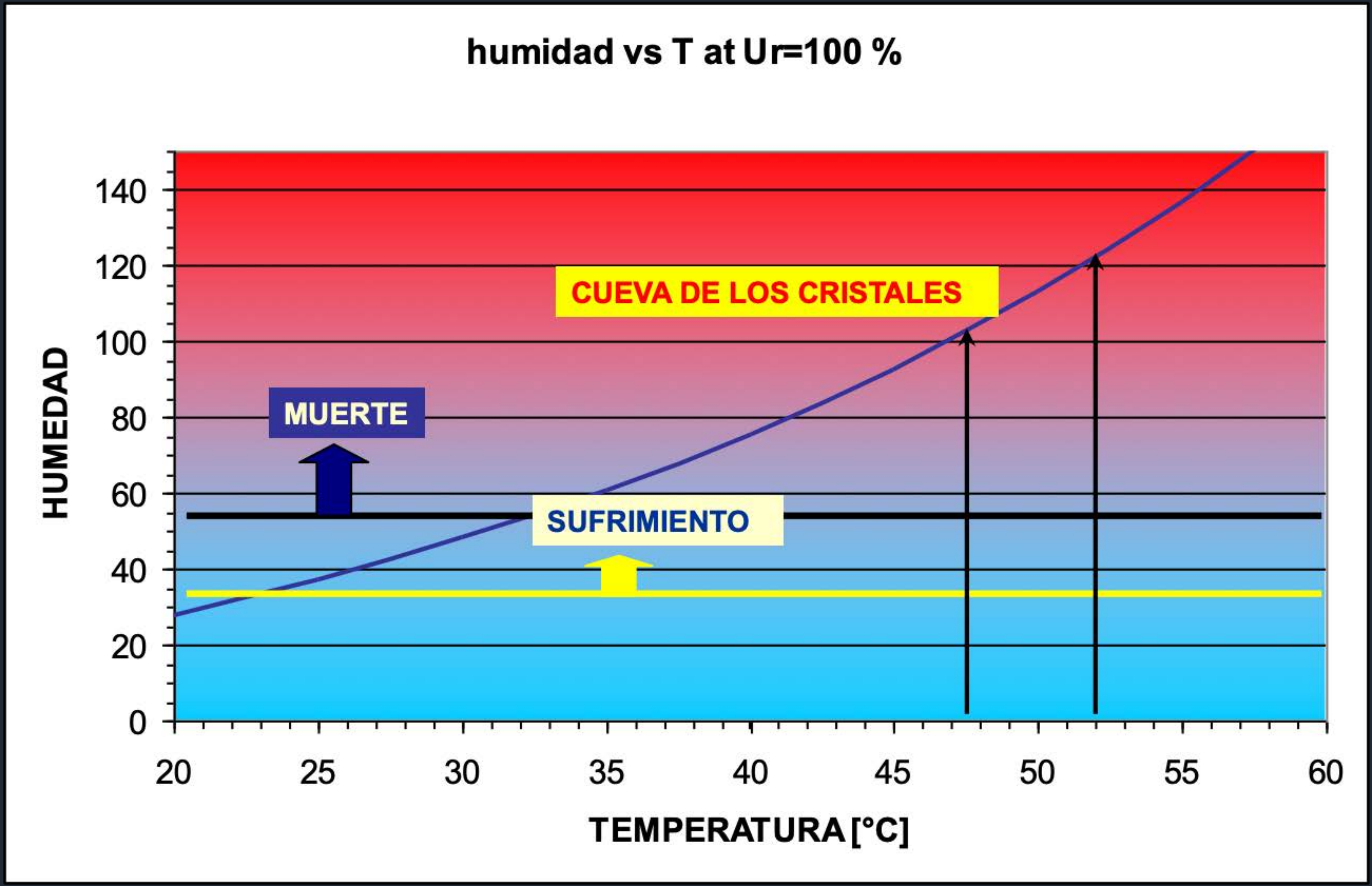


UTILIZACIÓN DE TRAJES ESPECIALES

A Cold Wall in a Hot-Wall Reactor

10 minutes

20 minutes

3-Temperature Technique

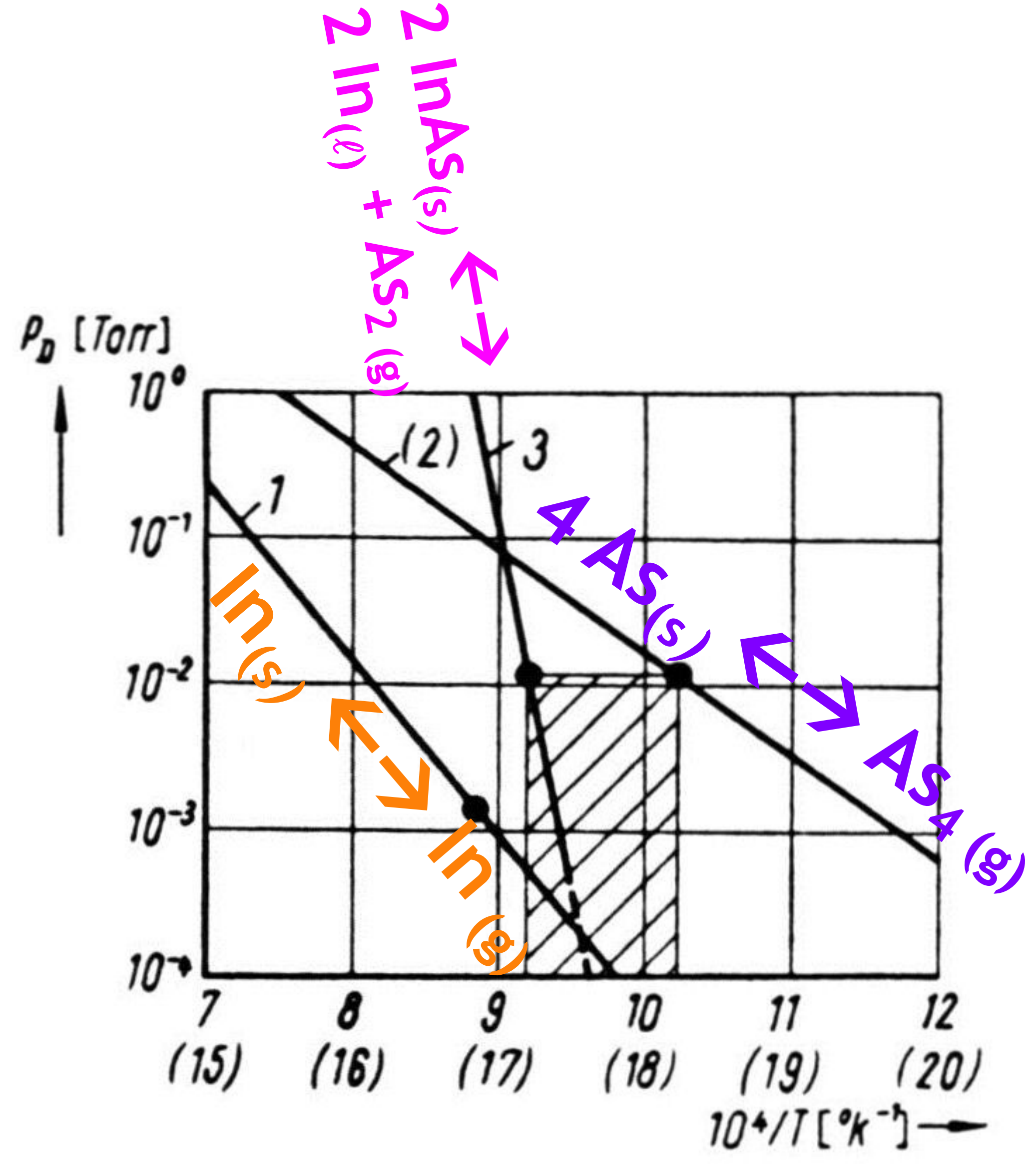

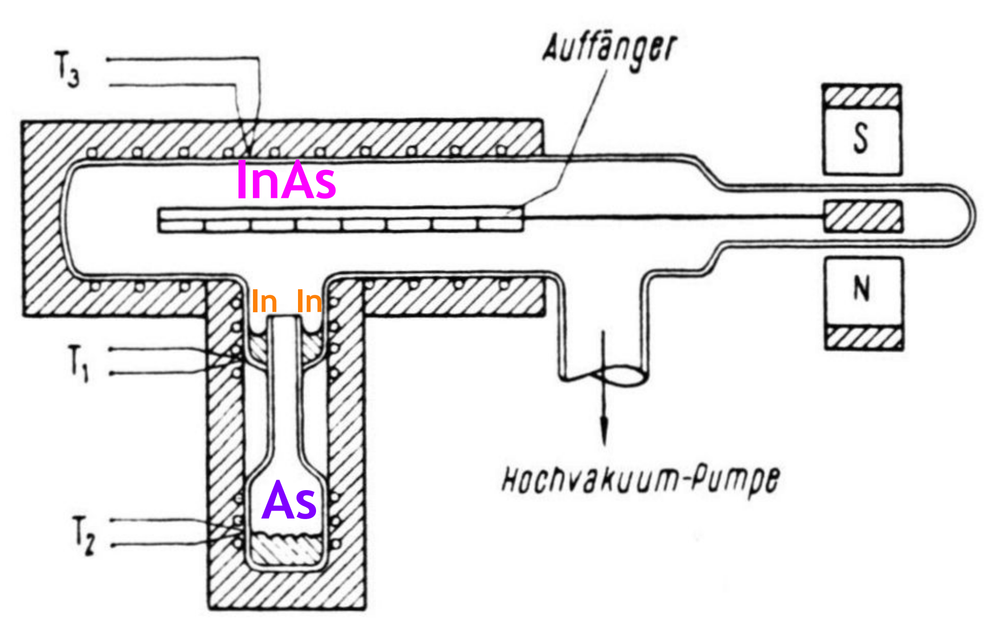

K.G. Günther, “Aufdampfschichten aus halbleitenden III-V Verbindungen,”
Zeitschrift für Naturforschung A **13** (1958) 1081–1089.

MBE also Works for Oxides—Properties

Material	Best MBE Figure of Merit	Best non-MBE Figure of Merit	References
ZnO	μ_e = 230,000 cm^2/(V·s) at 1 K	μ_e = 5,500 cm^2/(V·s) at 1 K	1,2
$SrTiO_3$	μ_e = 53,200 cm^2/(V·s) at 2 K	μ_e = 6,600 cm^2/(V·s) at 2 K	3,4
$EuTiO_3$	μ_e = 3,200 cm^2/(V·s) at 2 K	μ_e = 30 cm^2/(V·s) at 2 K	5,6
$SrSnO_3$	μ_e = 70 cm^2/(V·s) at 300 K	μ_e = 40 cm^2/(V·s) at 300 K	7,8
$BaSnO_3$	μ_e = 183 cm^2/(V·s) at 300 K	μ_e = 140 cm^2/(V·s) at 300 K	9,10
$CaRuO_3$	$R_{300\text{ K}} / R_{4\text{ K}} = 75$	$R_{300\text{ K}} / R_{4\text{ K}} = 42$	11,12
$SrRuO_3$	$R_{300\text{ K}} / R_{10\text{ K}} = 115$	$R_{300\text{ K}} / R_{10\text{ K}} = 14$	13,14
Sr_2RuO_4	$T_{\text{c,midpoint}} = 1.8$ K	$T_{\text{c,midpoint}} = 1.1$ K	15,16
$SrVO_3$	$R_{300\text{ K}} / R_{5\text{ K}} = 222$	$R_{300\text{ K}} / R_{5\text{ K}} = 2$	17,18
EuO	Metal-insulator transition $\Delta R/R=10^{11}$	Metal-insulator transition $\Delta R/R=5\times10^{4}$	19,20

[1] J. Falson, *Sci. Rep.* **6** (2016) 26598.
[2] A. Tsukazaki, *Science* **315** (2007) 1388-1391.
[3] T. A. Cain, *Appl. Phys. Lett.* **102** (2013) 182101.
[4] Y. Kozuka, *Appl. Phys. Lett.* **97** (2010) 012107.
[5] K. Maruhashi, *Adv. Mater.* **32** (2020) 1908315.
[6] K.S. Takahashi, *Phys. Rev. Lett.* **103** (2009) 057204.
[7] T. Truttmann, *Appl. Phys. Lett.* **115** (2019) 152103.
[8] E. Baba, *J. Phys. D: Appl. Phys.* **48** (2015) 455106.
[9] H. Paik, *APL Mater.* **5** (2017) 116107.
[10] A.P. Nono Tchiomo, *APL Mater.* **7** (2019) 041119.
[11] H.P. Nair, *APL Mater.* **6** (2018) 046101.
[12] S. Esser, *Eur. Phys. J. B* **87** (2014) 133.
[13] H. Nair, presented at Spring MRS Meeting (2019).
[14] D. Kan, *J. Appl. Phys.* **113** (2013) 173912.
[15] H.P. Nair, *APL Mater.* 6 (2018) 101108.
[16] J. Kim, *Nano Lett.* **21** (2021) 4185–4192.
[17] J.A. Moyer, *Adv. Mater.* **25** (2013) 3578-3582.
[18] W.C. Sheets, *Appl. Phys. Lett.* **91** (2007) 192102.
[19] D.V. Averyanov, *Nanotechnology* **29** (2018) 195706.
[20] T. Yamasaki, *Appl. Phys. Lett.* **98** (2011) 082116.

Adsorption-Controlled Growth of GaAs

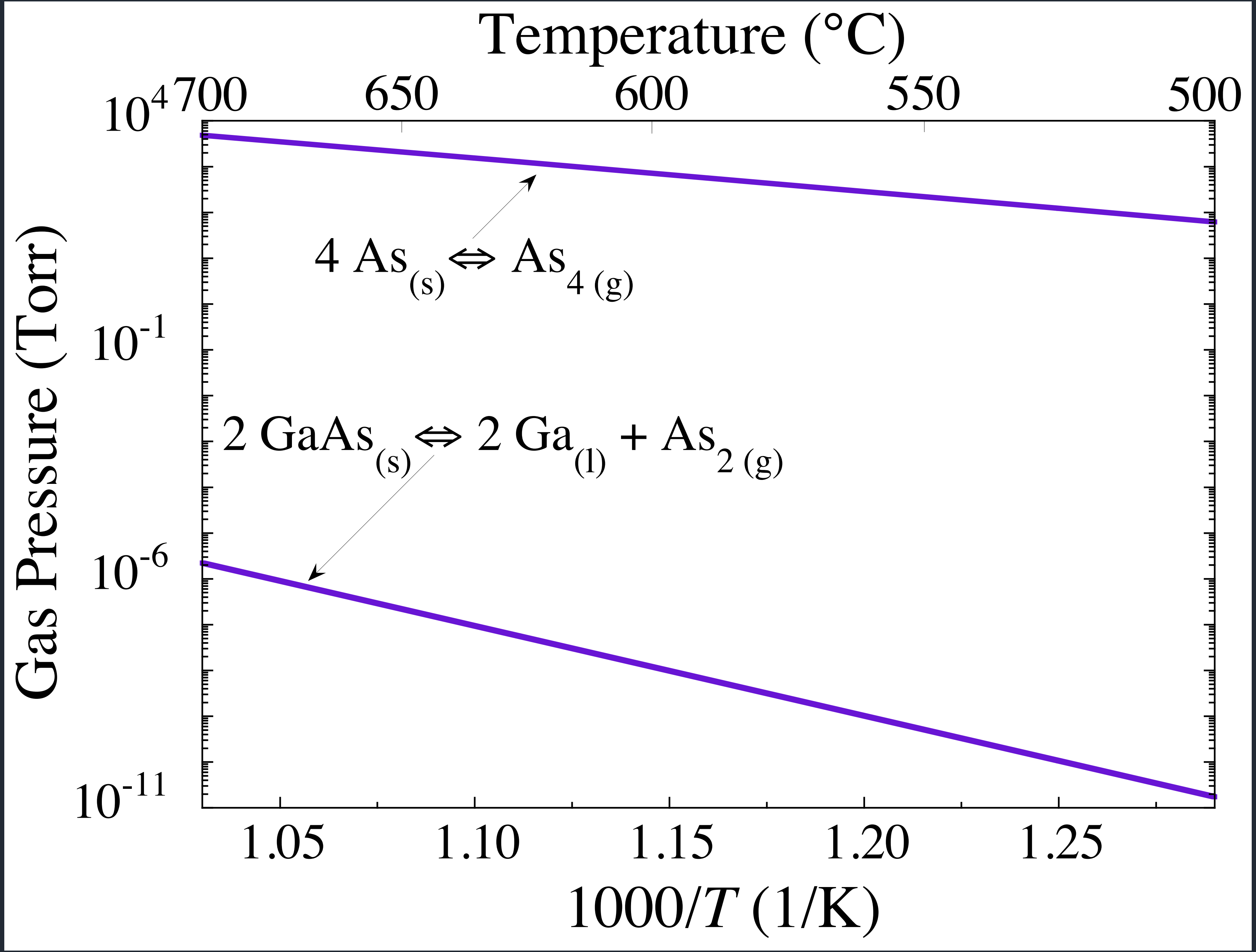

C.D. Theis, J. Yeh, D.G. Schlom, M.E. Hawley, and G.W. Brown, "Adsorption-Controlled Growth of $PbTiO_3$ by Reactive Molecular Beam Epitaxy," *Thin Solid Films* **325** (1998) 107-114.

Adsorption-Controlled Growth of $PbTiO_3$

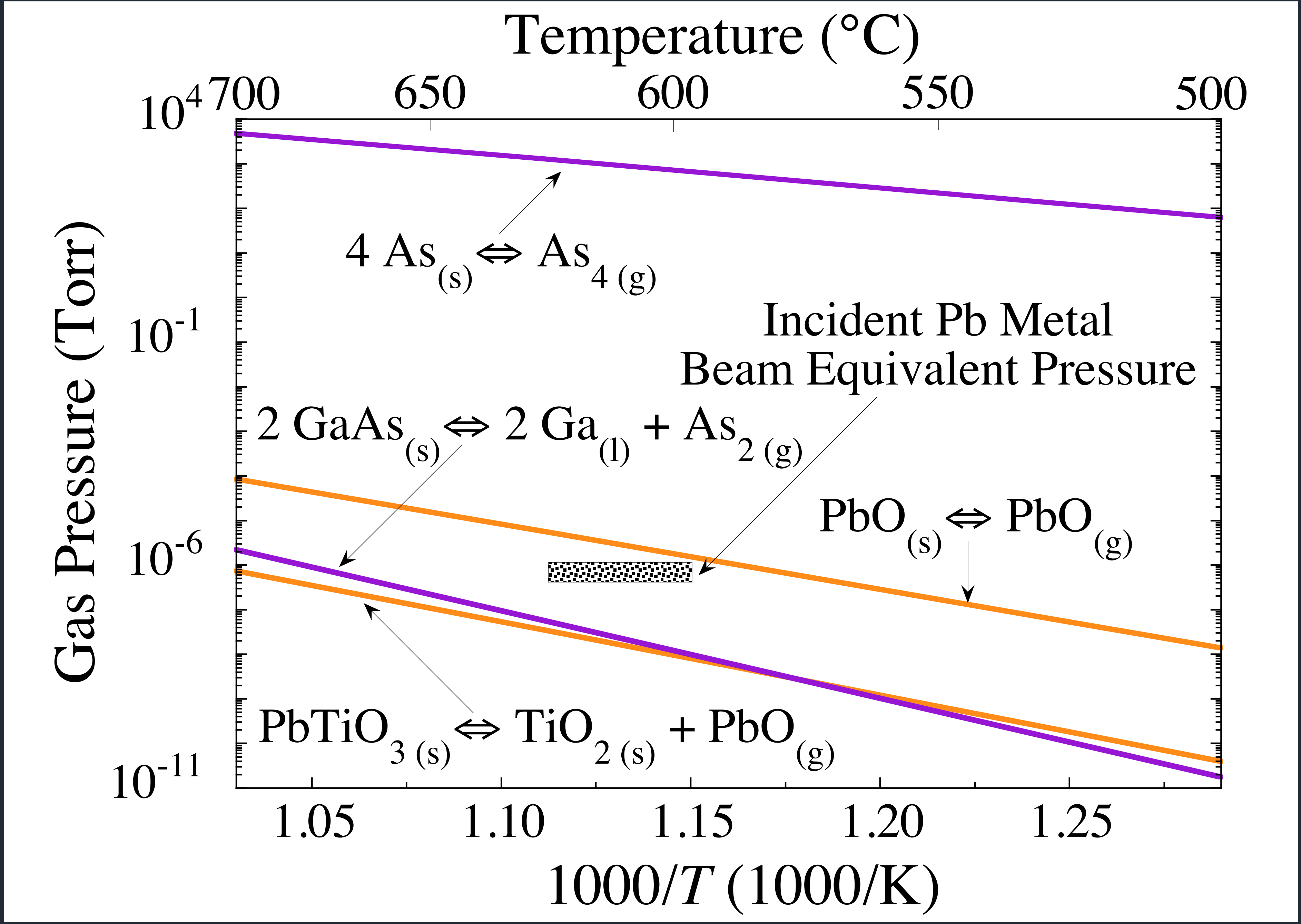

C.D. Theis, J. Yeh, D.G. Schlom, M.E. Hawley, and G.W. Brown, "Adsorption-Controlled Growth of $PbTiO_3$ by Reactive Molecular Beam Epitaxy," *Thin Solid Films* **325** (1998) 107-114.

Adsorption-Controlled Growth of $PbTiO_3$

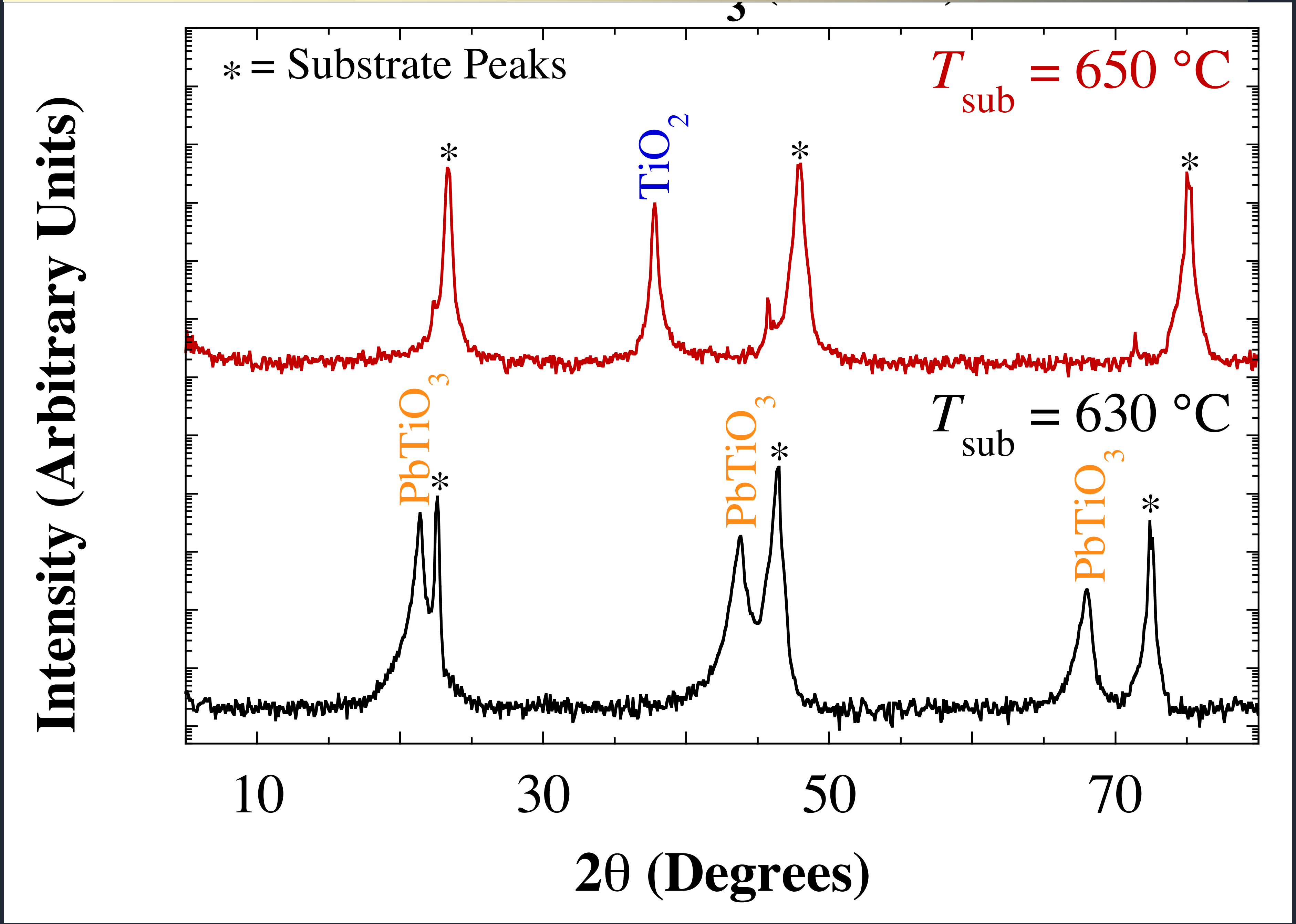

Adsorption-Controlled Growth of

- Plumbites
  - $PbTiO_3$ — C.D. Theis *et al.*, *J. Cryst. Growth* **174** (1997) 473-479.
  - $PbZrO_3$ — (unpublished)

- Bismuthates
  - $Bi_2Sr_2CuO_6$ — S. Migita *et al.*, *Appl. Phys. Lett.* **71** (1997) 3712-3714.
  - $Bi_4Ti_3O_{12}$ — C.D. Theis *et al.*, *Appl. Phys. Lett.* **72** (1998) 2817-2819.
  - $BiFeO_3$ — J.F. Ihlefeld *et al.*, *Appl. Phys. Lett.* **91** (2007) 071922.
  - $BiMnO_3$ — J.H. Lee *et al.*, *Appl. Phys. Lett.* **96** (2010) 262905.
  - $BiVO_4$ — S. Stoughton *et al.*, *APL Materials* **1** (2013) 042112.
  - $Bi_2Sn_2O_7$ and $Bi_2Ru_2O_7$ — (unpublished)

- Ferrites
  - $LuFe_2O_4$ — C.M. Brooks *et al.*, *Appl. Phys. Lett.* **101** (2012) 132907.

Adsorption-Controlled Growth of

- **Ruthenates**
  - $SrRuO_3$ — D.E. Shai *et al.*, *Phys. Rev. Lett.* **110** (2013) 087004.
  - Ba_2RuO_4 — B. Burganov *et al.*, *Phys. Rev. Lett.* **116** (2016) 197003.
  - $CaRuO_3$ — H.P. Nair *et al.*, *APL Mater.* **6** (2018) 046101.
  - Sr_2RuO_4 — H.P. Nair *et al.*, *APL Mater.* **6** (2018) 101108.
  - Ca_2RuO_4 — (unpublished)
- **Iridates**
  - Ba_2IrO_4 — M. Uchida *et al.*, *Phys. Rev. B* **90** (2014) 075142.
  - $SrIrO_3$ and Sr_2IrO_4 — Y.F. Nie *et al.*, *Phys. Rev. Lett.* **114** (2015) 016401.
- **Stannates**
  - $BaSnO_3$ — H. Paik *et al.*, *APL Materials* **5** (2017) 116107.
- **Other**
  - EuO — R.W. Ulbricht *et al.*, *Appl. Phys. Lett.* **93** (2008) 102105.

Adsorption-Controlled Growth of

- Titanates by MOMBE
  - $SrTiO_3$ – B. Jalan *et al.*, *Appl. Phys. Lett.* 95 (2009) 032906.
  - $GdTiO_3$ – P. Moetakef *et al.*, *J. Vac. Sci. Technol. A* **31** (2013) 041503.
  - $BaTiO_3$ – Y. Matsubara *et al.*, *Appl. Phys. Express* **7** (2014) 125502.
  - $CaTiO_3$ – R.C. Haislmaier *et al.*, *Adv. Funct. Mater.* **26** (2016) 7271.

- Vanadates by MOMBE
  - $LaVO_3$ – H.-T. Zhang *et al.*, *Appl. Phys. Lett.* **106** (2015) 233102.
  - $(La,Sr)VO_3$ – M. Brahlek *et al.*, *Appl. Phys. Lett.* **109** (2016) 101903.

- Stannates by MOMBE
  - $SrSnO_3$ – T. Wang *et al.*, *Phys Rev Mater.* **1** (2017) 061601.
  - $BaSnO_3$ – A. Prakash *et al.*, *J. Mater. Chem. C* **5** (2017) 5730.

Adsorption-Controlled Growth of

- **Stannates by Suboxide MBE**
  - **SnO** – A.B. Mei *et al.*, *Phys. Rev. Mater.* **3** (2019) 105202.
  - **Sr_3SnO** – Y. Ma *et al. Adv. Mater.* **32** (2020) 2000809.
  - **Ta_2SnO_6** – M. Barone *et al. J. Phys. Chem. C* **126** (2022) 3764–3775.
- **Gallates by Suboxide MBE**
  - **Ga_2O_3** – P. Vogt *et al.*, *APL Mater.* **9** (2021) 031101.
- **Indates by Suboxide MBE**
  - **In_2O_3** – P. Vogt *et al.*, *Phys. Rev. Appl.* **17** (2022) 034021 .

Adsorption-Controlled Growth of $Bi_4Ti_3O_{12}$

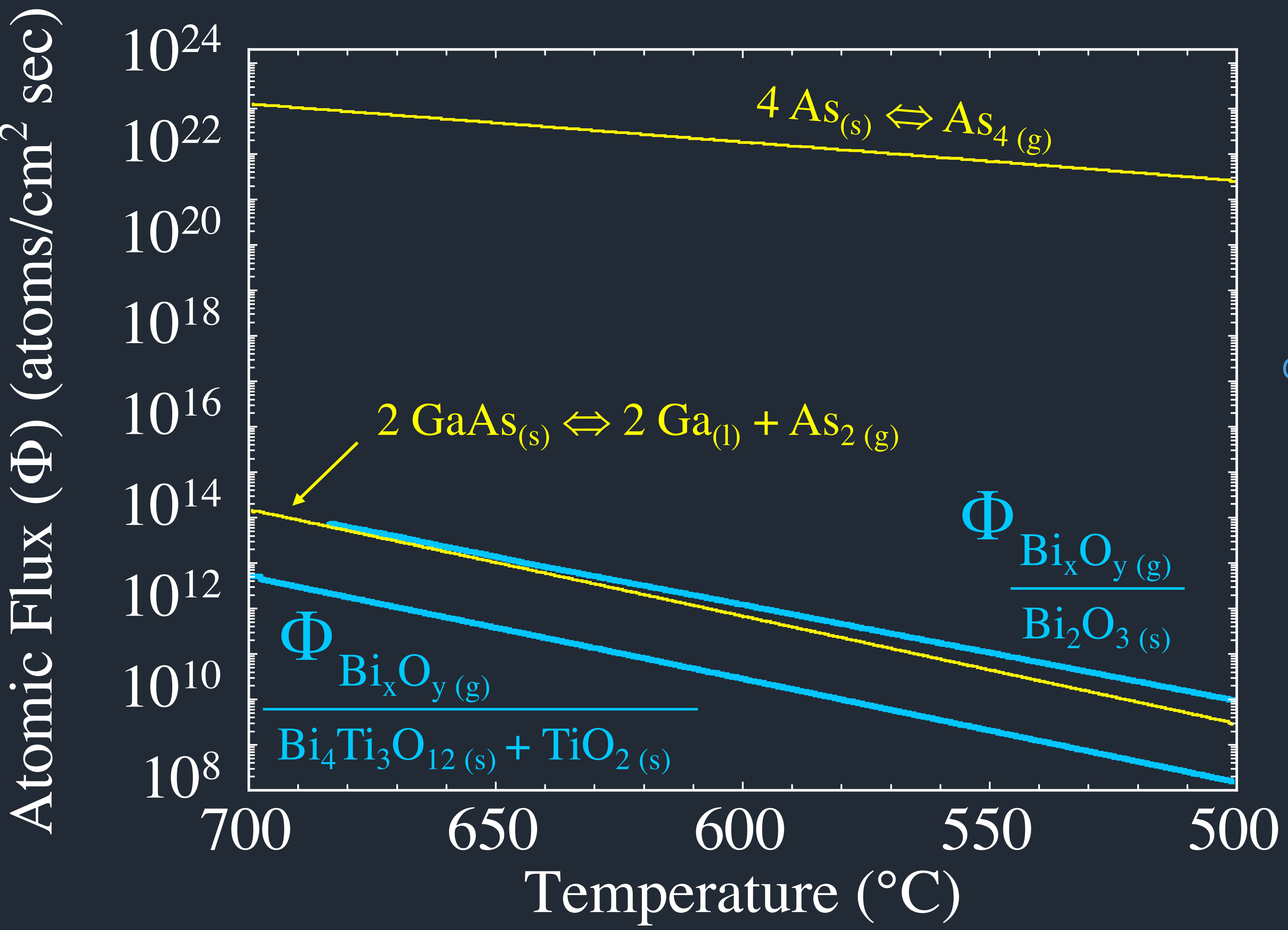

D.G. Schlom, J.H. Haeni, J. Lettieri,
C.D. Theis, W. Tian, J.C. Jiang, and X.Q. Pan,
Mater. Sci. Eng. ***B*** **87** (2001) 282-291.

Adsorption-Controlled Growth of $Bi_4Ti_3O_{12}$

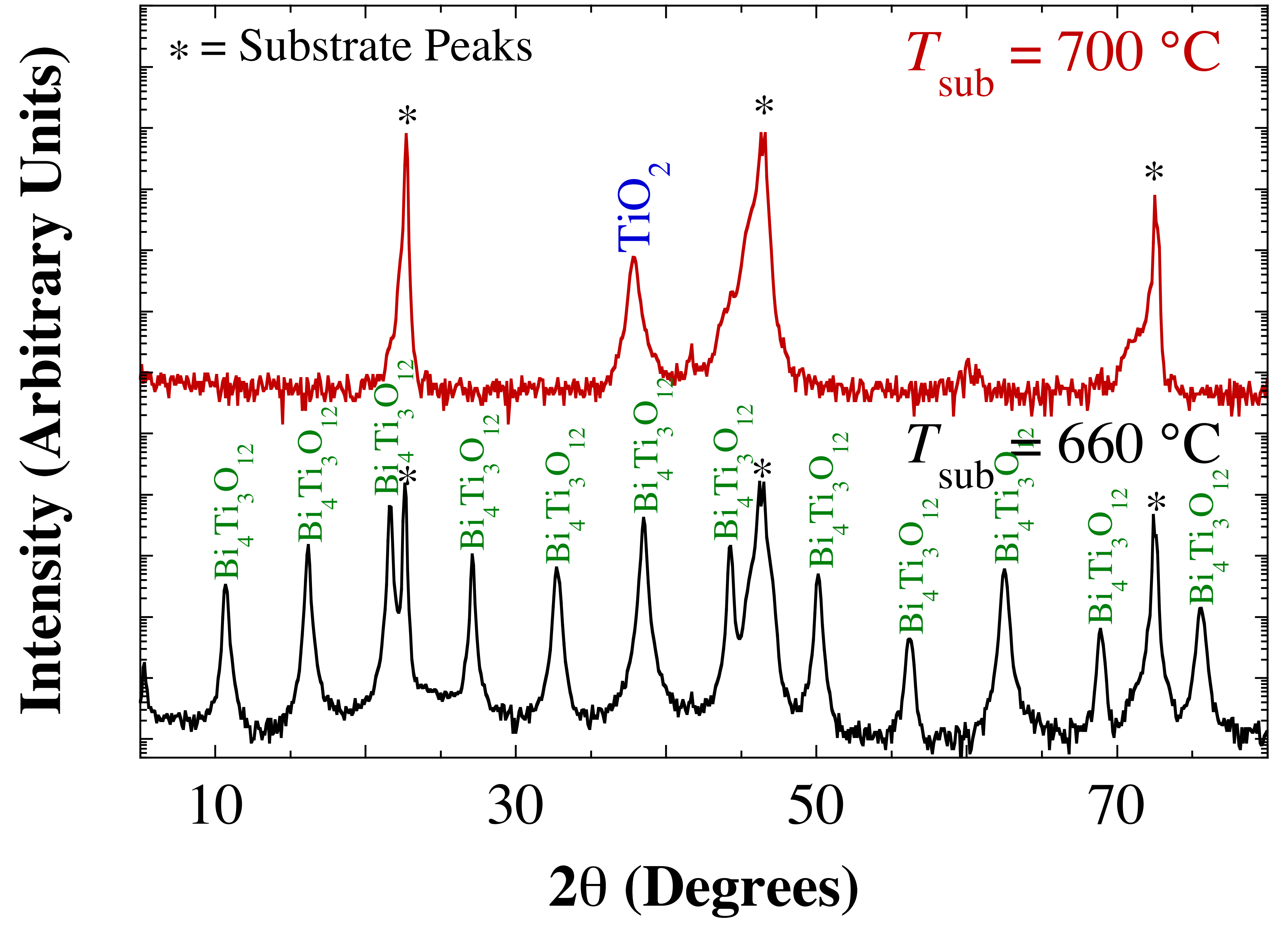

Adsorption-Controlled Growth of $Bi_4Ti_3O_{12}$

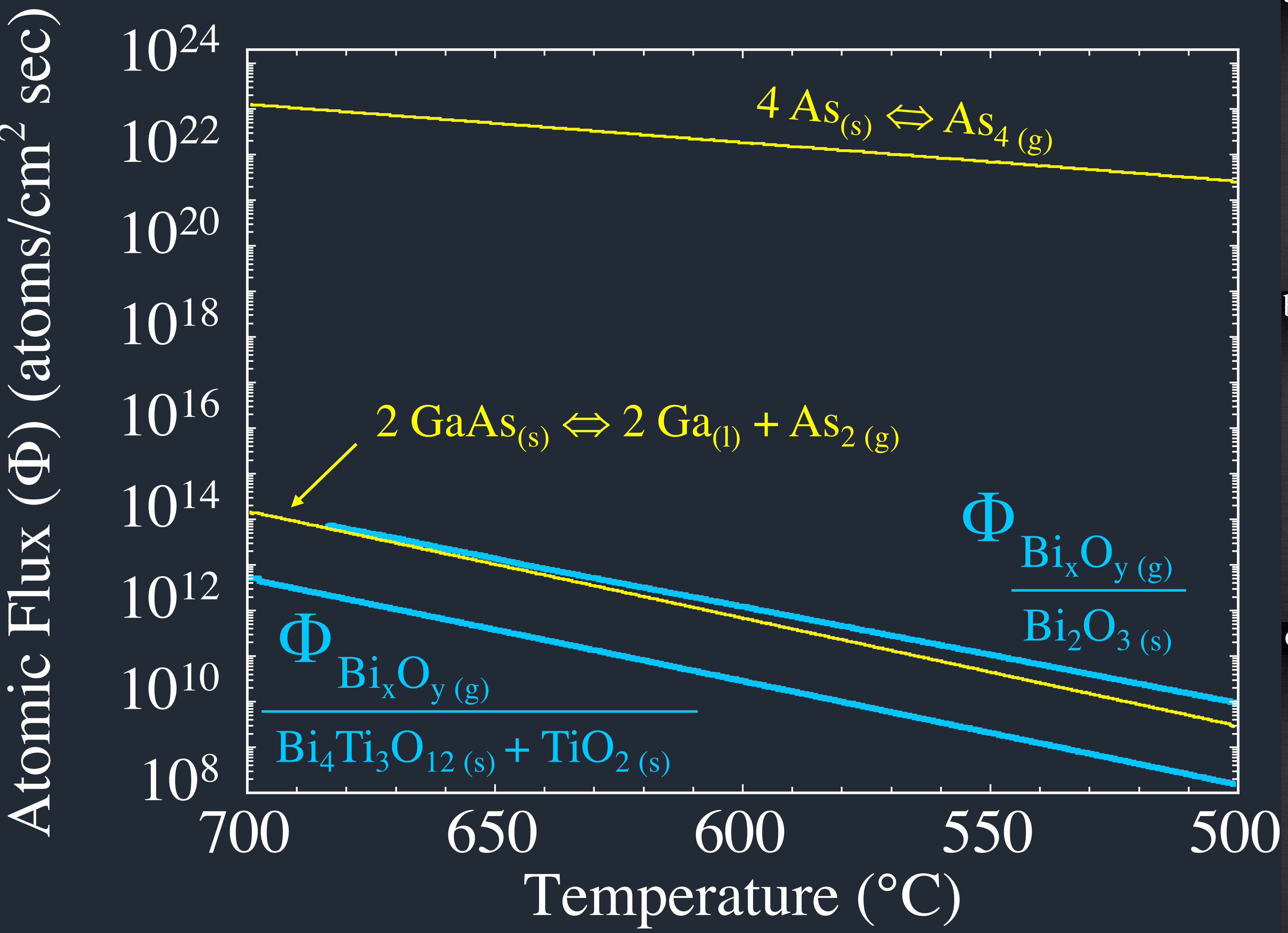

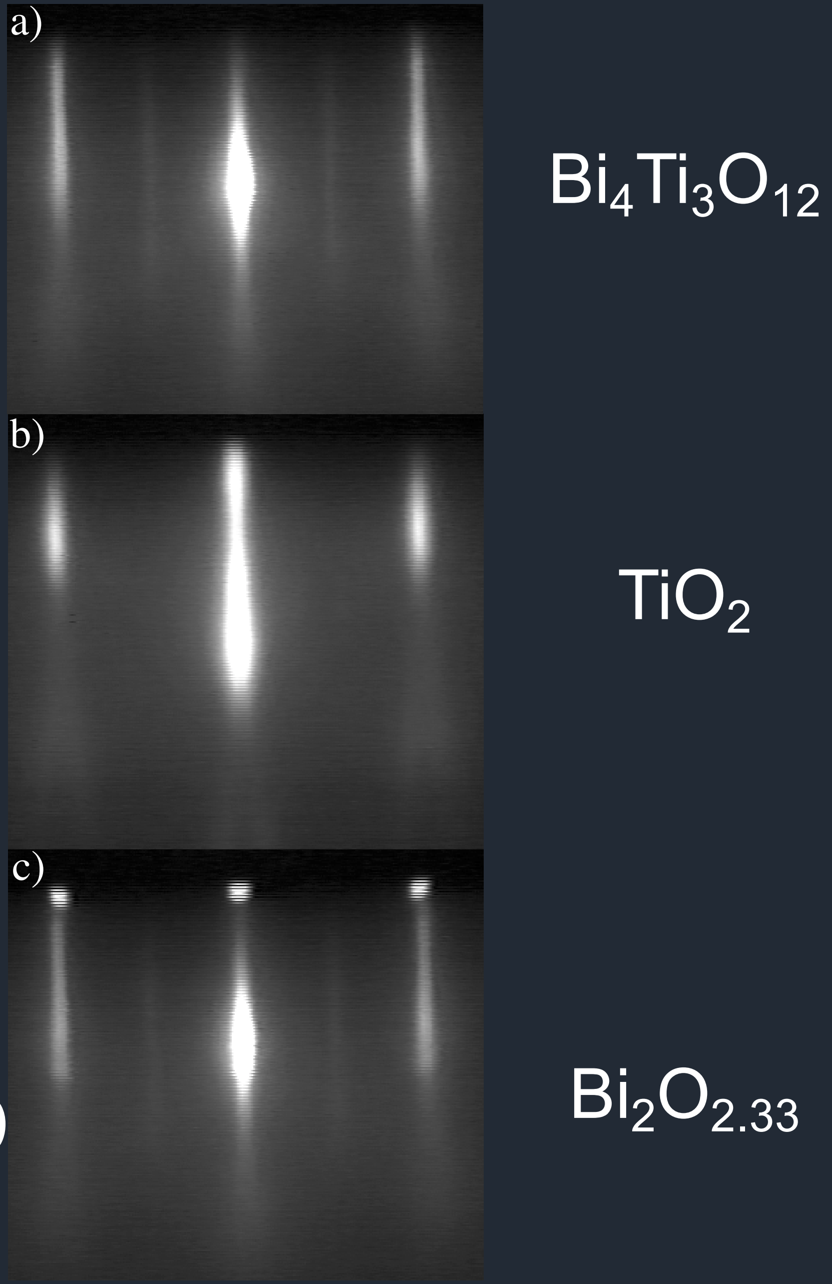

Adsorption-Controlled Growth of $BaSnO_3$

H. Paik, Z. Chen, E. Lochocki, A. Seidner H., A. Verma, N. Tanen, J. Park, M. Uchida, S.L. Shang, B-C. Zhou, M. Brützam, R. Uecker, Z.K. Liu, D. Jena, K.M. Shen, D.A. Muller, and D.G. Schlom, *APL Materials* **5** (2017) 116107.

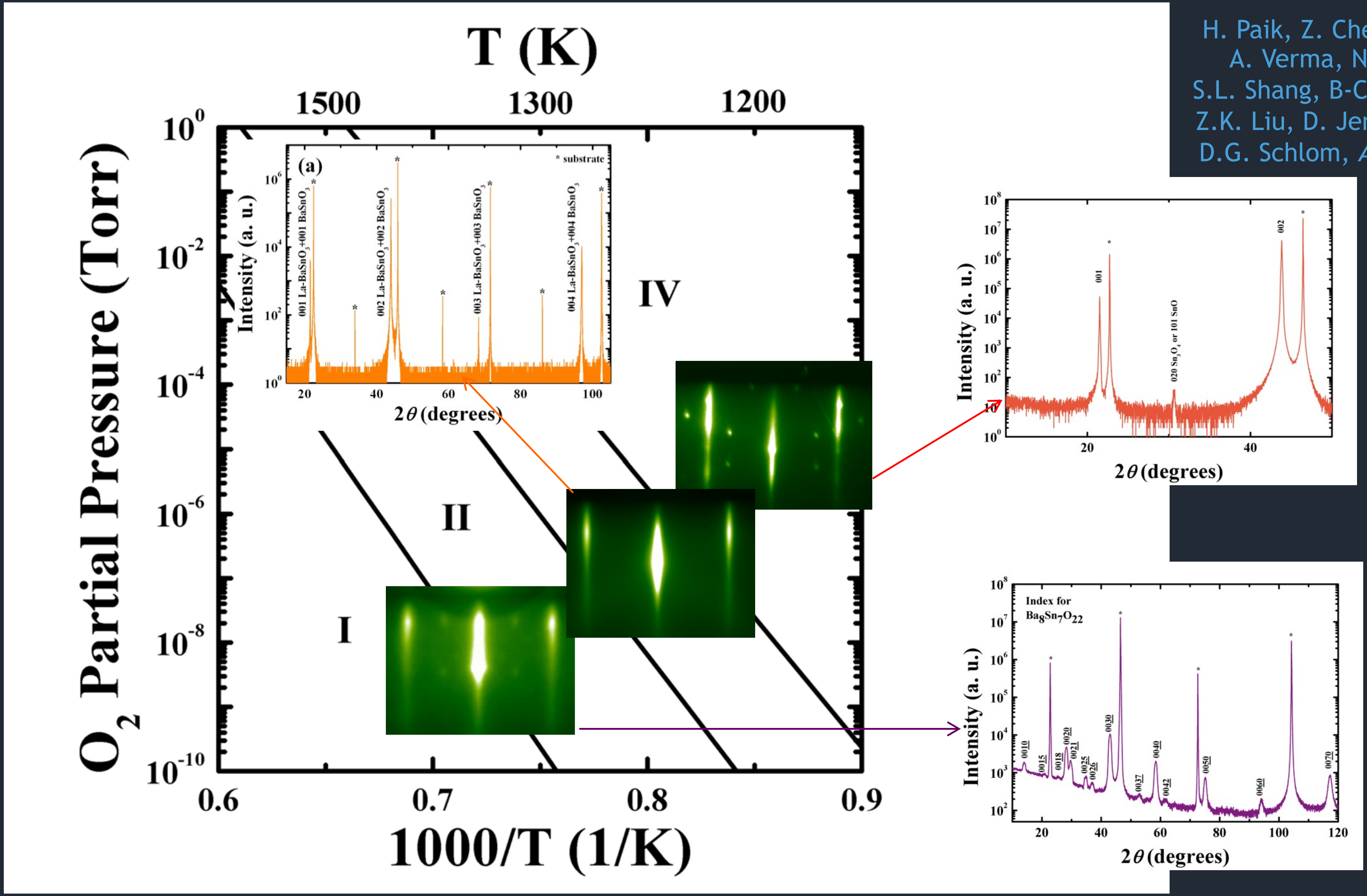

Adsorption-Controlled Growth of EuO

Eu Flux = 1.1×10^{14} Eu atoms/(cm^2 s), T_{sub} = 590 ° C

EuO film thickness (from RBS) after 30 min

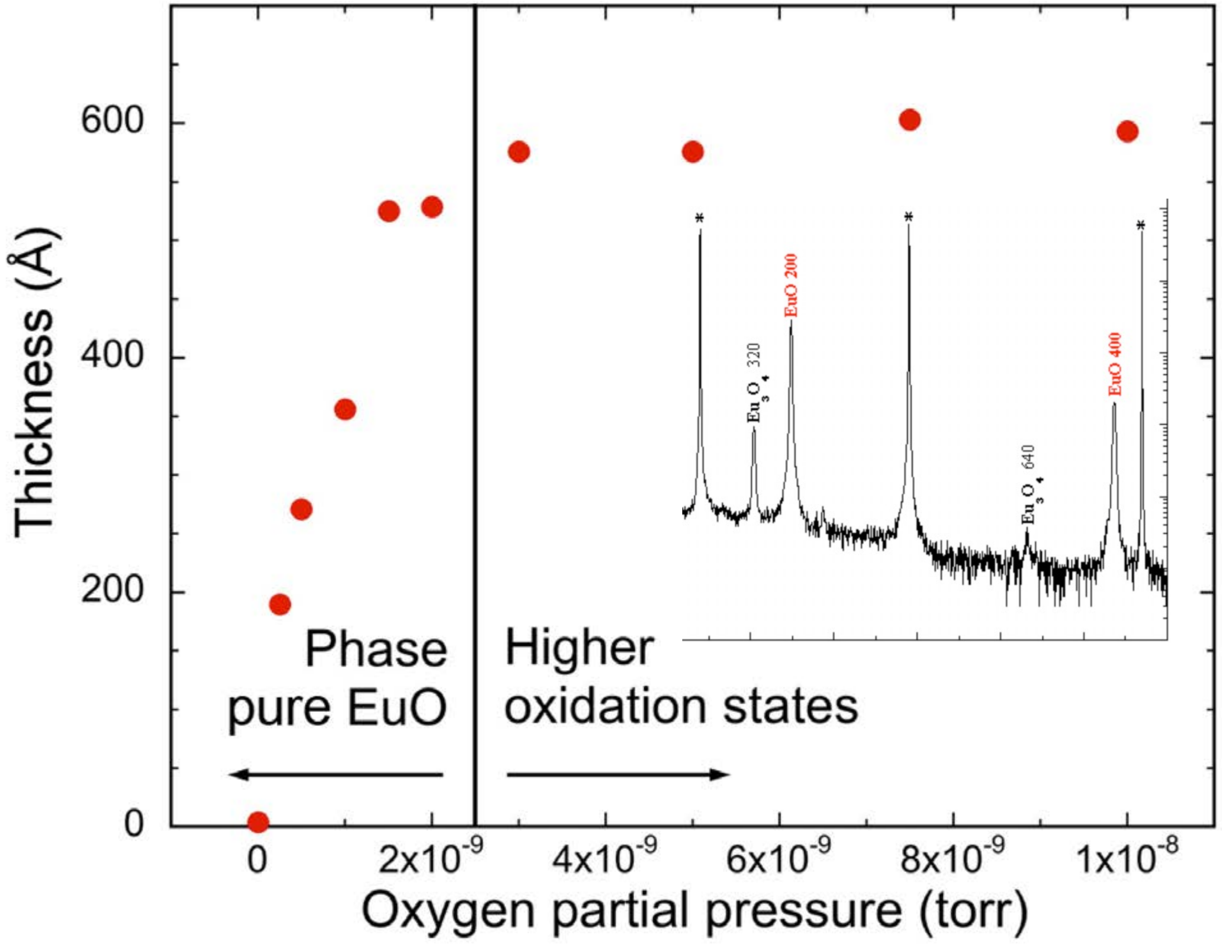

R.W. Ulbricht, A. Schmehl, T. Heeg, J. Schubert, and D.G. Schlom,
Applied Physics Letters **93** (2008) 102105.

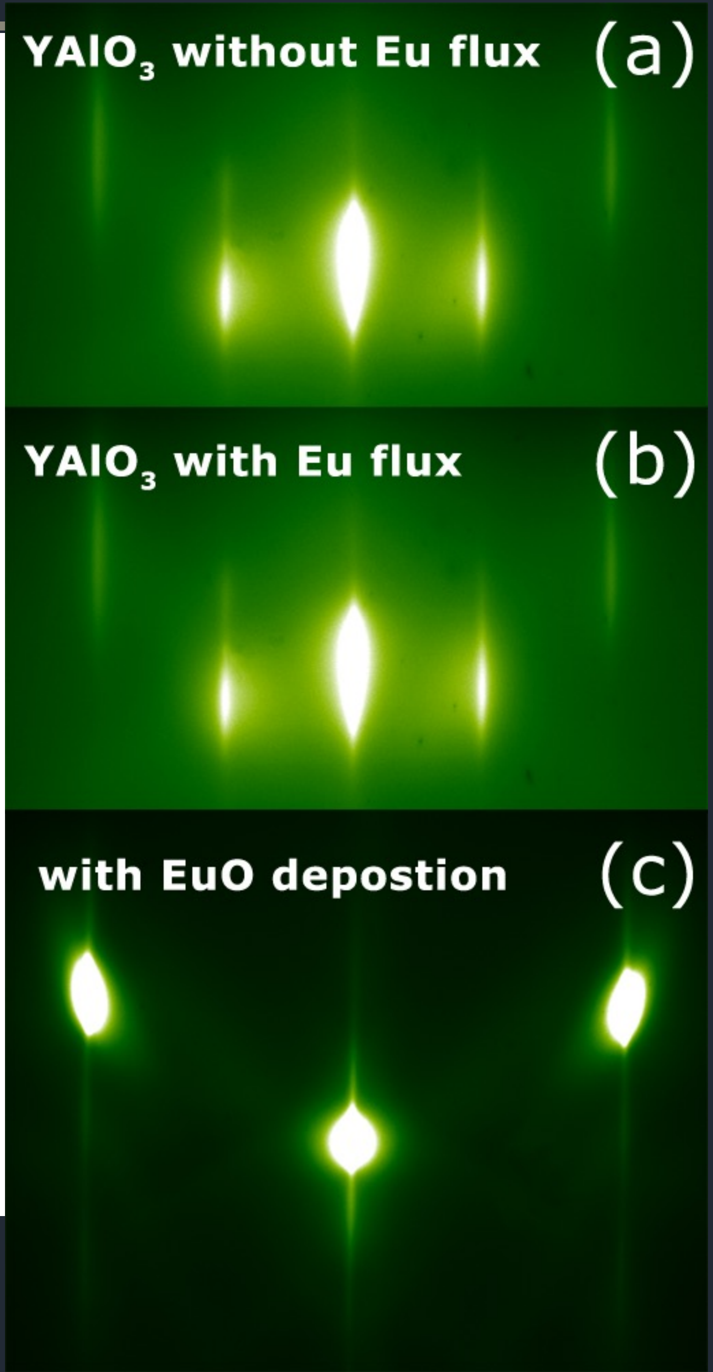

Adsorption-Controlled Growth of $SrTiO_3$

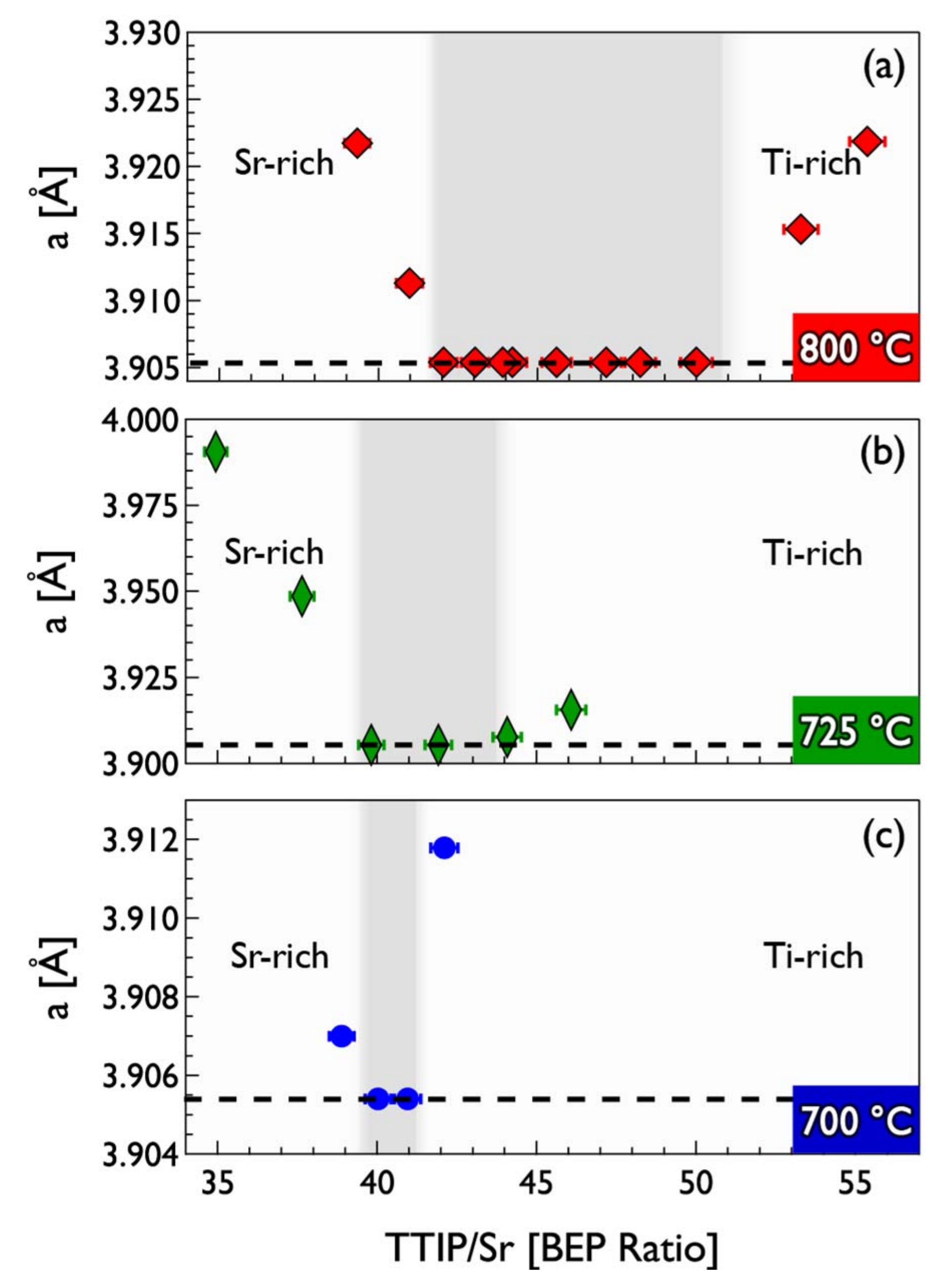

MOMBE Sources

Sr

$Ti(OC_3H_7)_4$

Oxygen Plasma

B. Jalan, P. Moetakef, and S. Stemmer,
Applied Physics Letters **95** (2009) 032906.

Single-Phase Field of GaAs vs. $PbTiO_3$

$PbTiO_3$

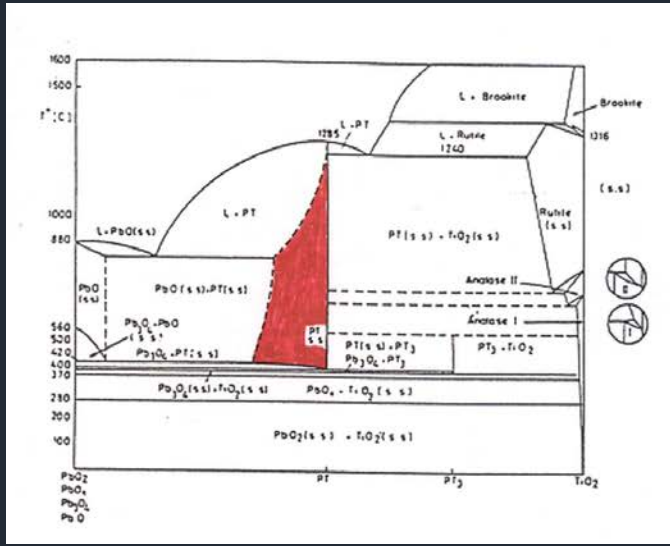

M.A. Eisa, M.F. Abadir, and A.M. Gadalla,
Transactions and Journal of
the British Ceramic Society **79** (1980) 100–104.

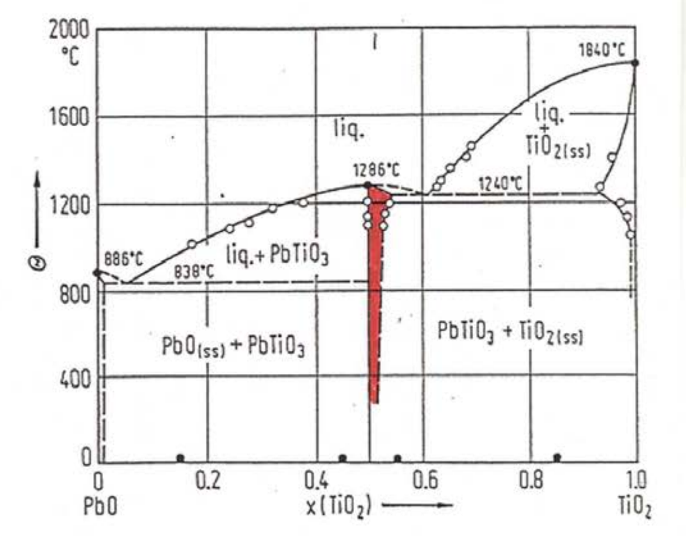

R.L. Holman
Ferroelectrics **14** (1976) 675–678.

GaAs

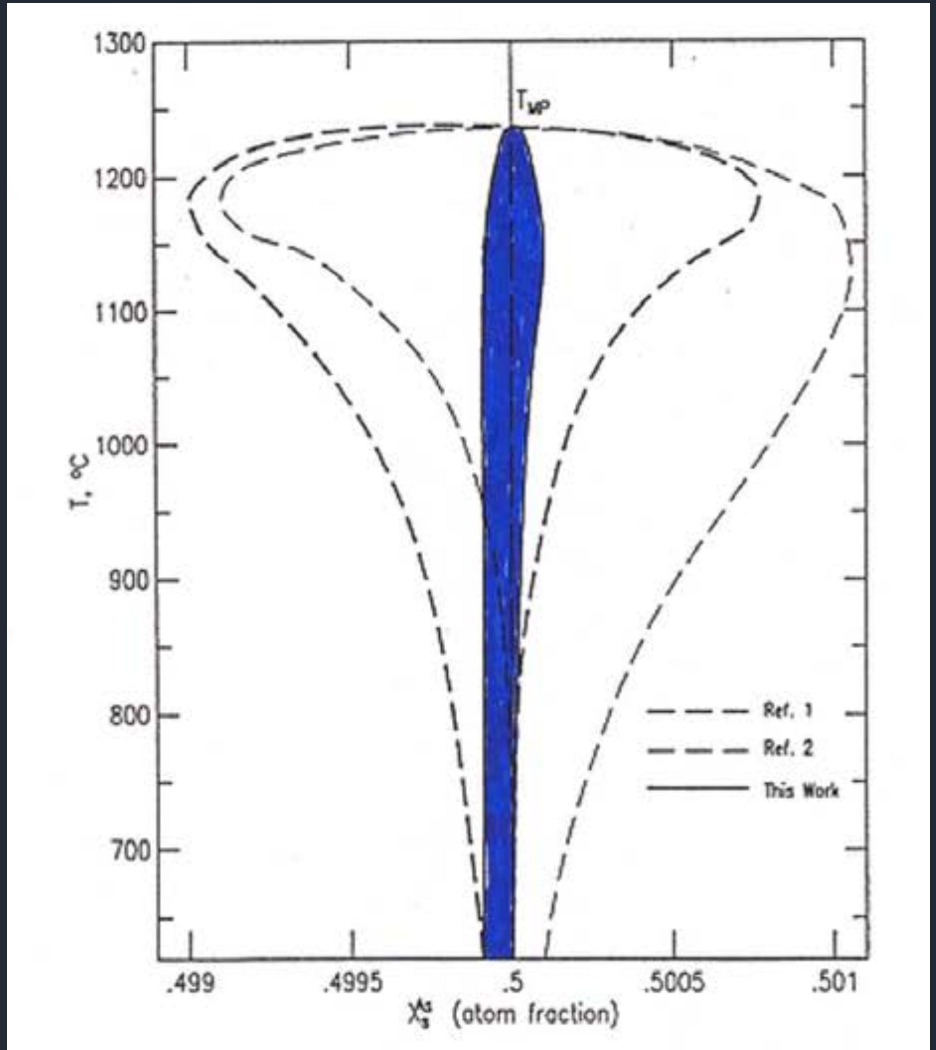

Fig. 8337—GaAs solidus curve. Curves represent the calculated deviations from stoichiometry for solid GaAs.
A. I. Ivashchenko, F. Ya. Kopanskaya, and G. S. Kuzmenko, *J. Phys. Chem. Solids*, 45 [8-9] 871-875 (1984).

Single-phase film does not imply stoichiometric film

Phase Diagrams for Ceramists, Vol. 9, edited by G.B. Stringfellow (American Ceramic Society, Westerville, 1992) p. 126.

Thermodynamics of Sr_2RuO_4 by MBE

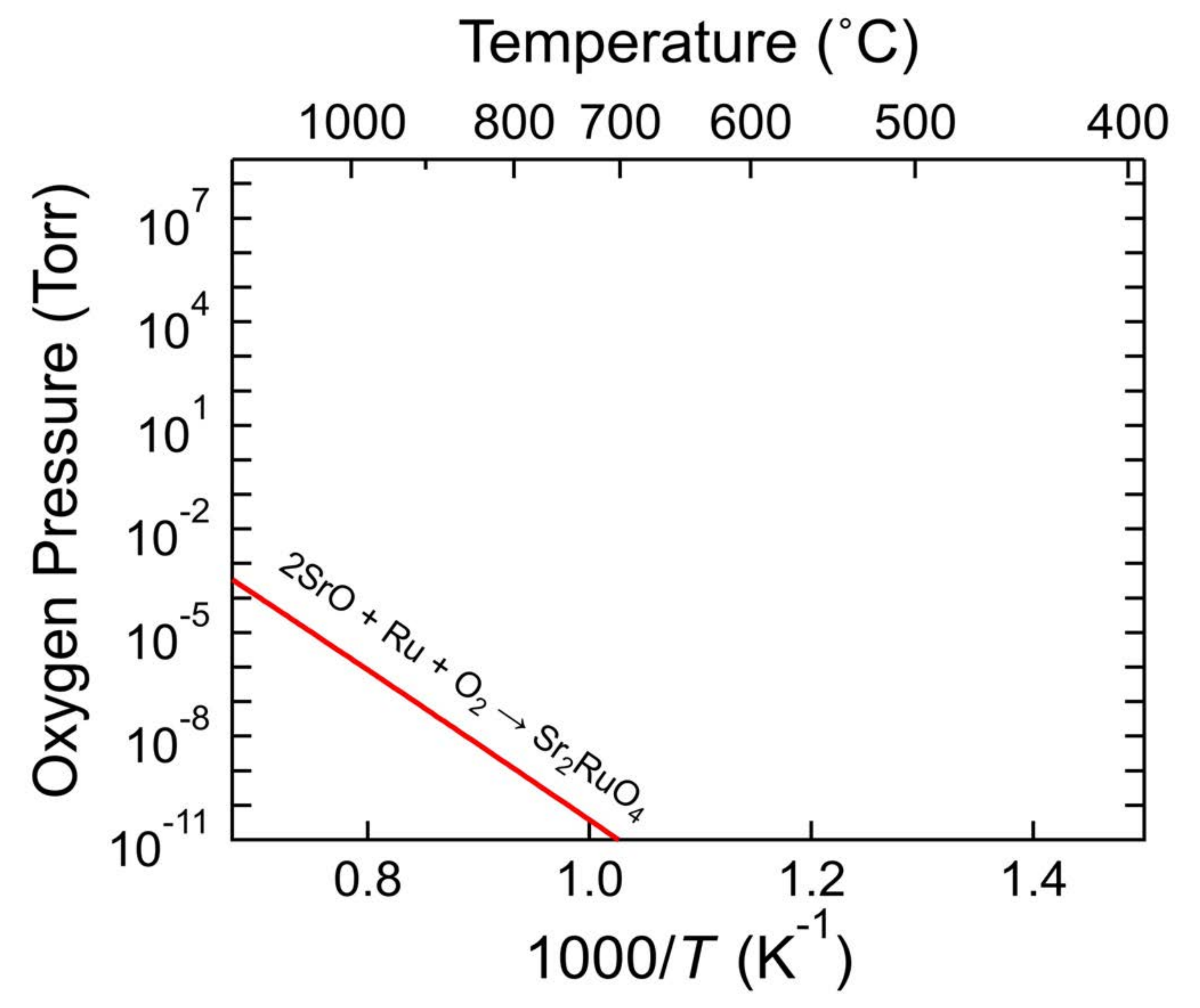

Thermodynamic data from: K.T. Jacob, K.T. Lwin, and Y. Waseda,
J. Mater. Sci. Eng., B **103** (2003) 152–161.

Thermodynamics of Sr_2RuO_4 by MBE

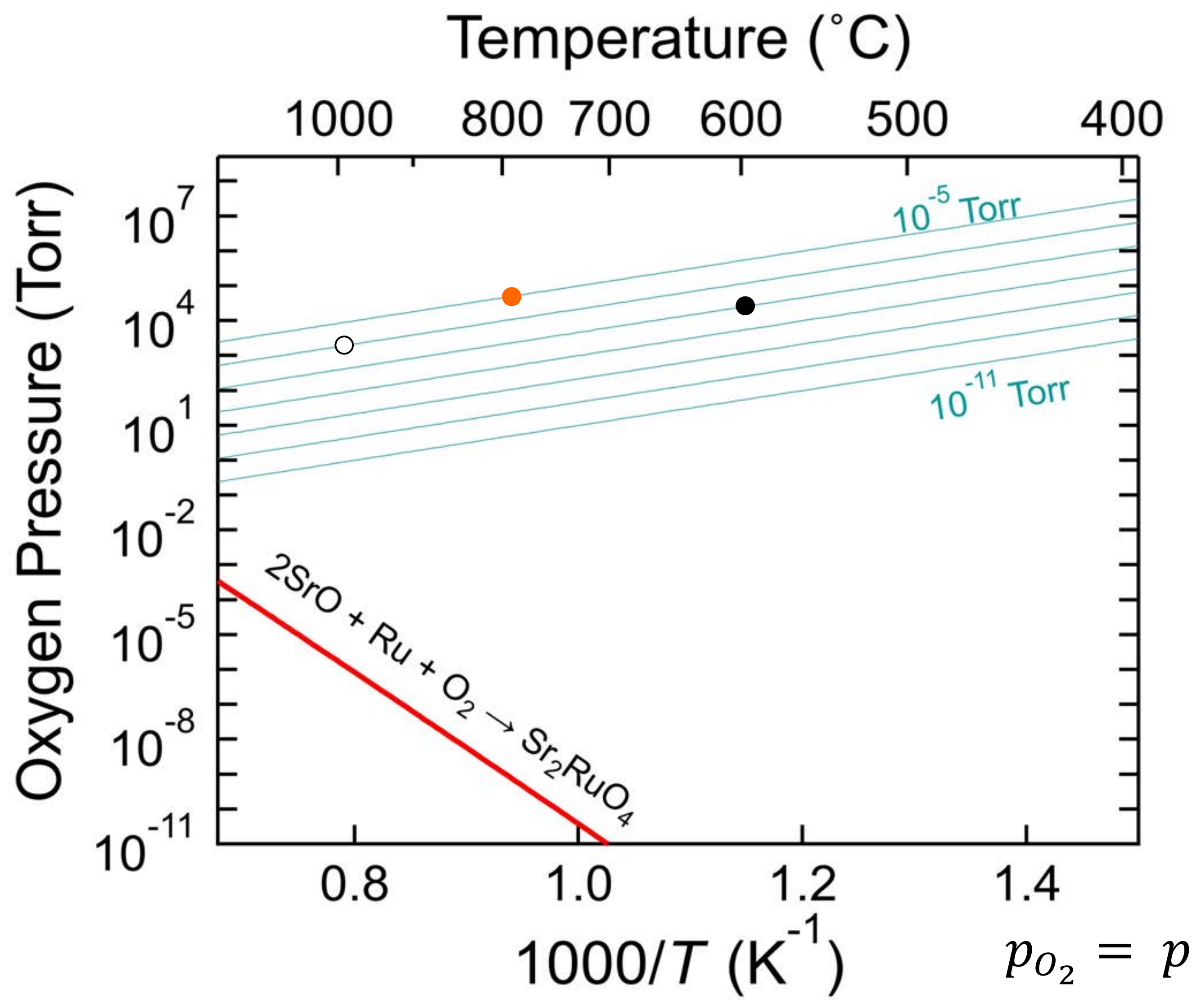

- ● T_s = 600 ˚C
  p_{O_3} = 10^{-7} Torr
- ○ T_s = 1000 ˚C
  p_{O_3} = 10^{-6} Torr
- ● T_s = 800 ˚C
  p_{O_3} = 10^{-5} Torr

$$O_2 \xrightarrow{\Delta G^\circ} \frac{2}{3} O_3$$

$$p_{O_2} = p_{O_3}{}^{2/3} \exp\left[\frac{\Delta G_0}{RT_s}\right]$$

Ozone decomposition thermodynamic calculation:
Y. Krockenberger, J. Kurian, A. Winkler, A. Tsukada, M. Naito, and L. Alff, *Phys. Rev. B* **77** (2008) 060505.

Thermodynamics of $Sr_{n+1}Ru_nO_{3n+1}$ by MBE

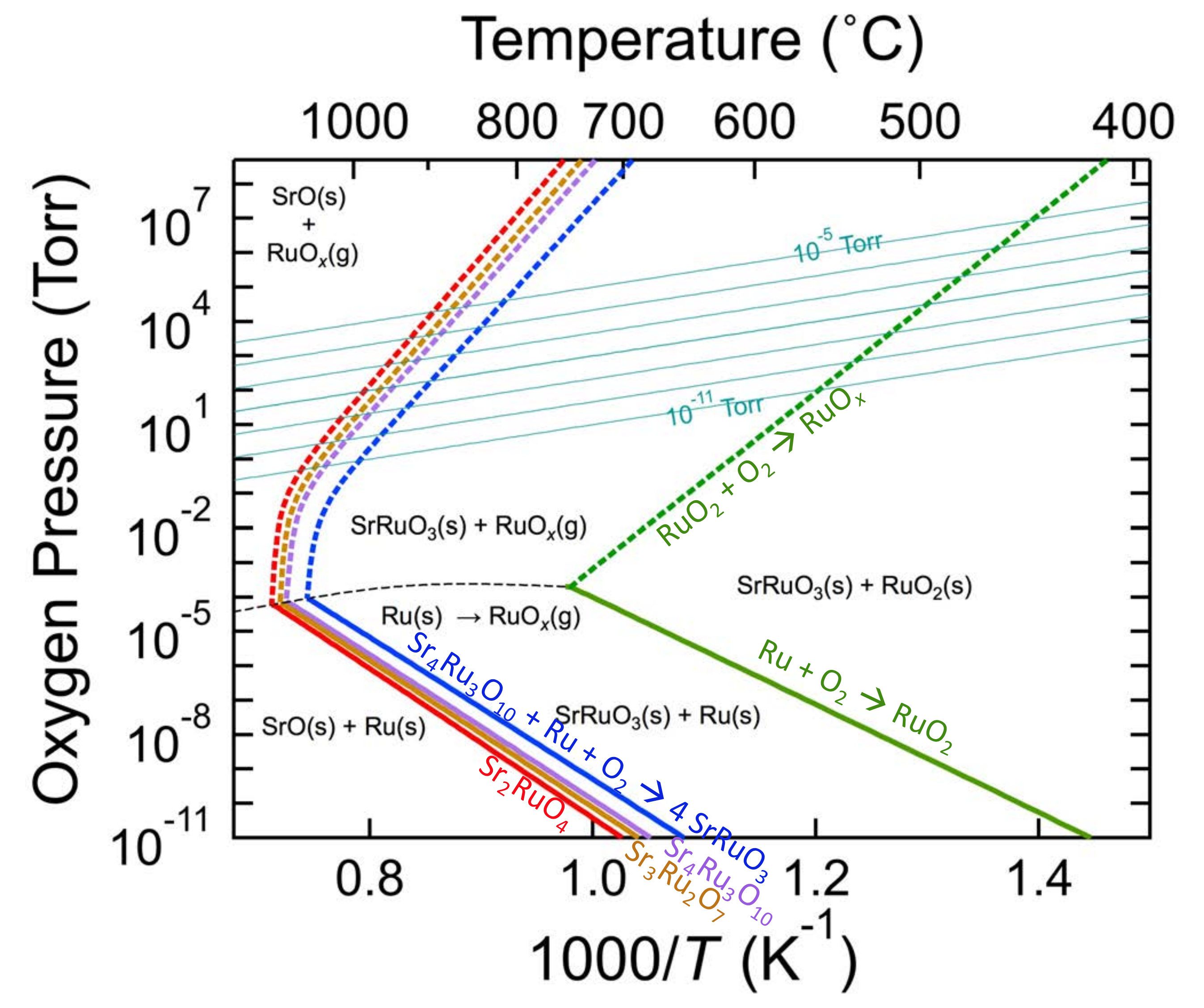

H.P. Nair, Y. Liu, J.P. Ruf, N.J. Schreiber, S-L. Shang, D.J. Baek, B.H. Goodge,
L.F. Kourkoutis, Z.K. Liu, K.M. Shen, and D.G. Schlom,
APL Materials **6** (2018) 046101.

Thermodynamics of $Sr_{n+1}Ru_nO_{3n+1}$ by MBE

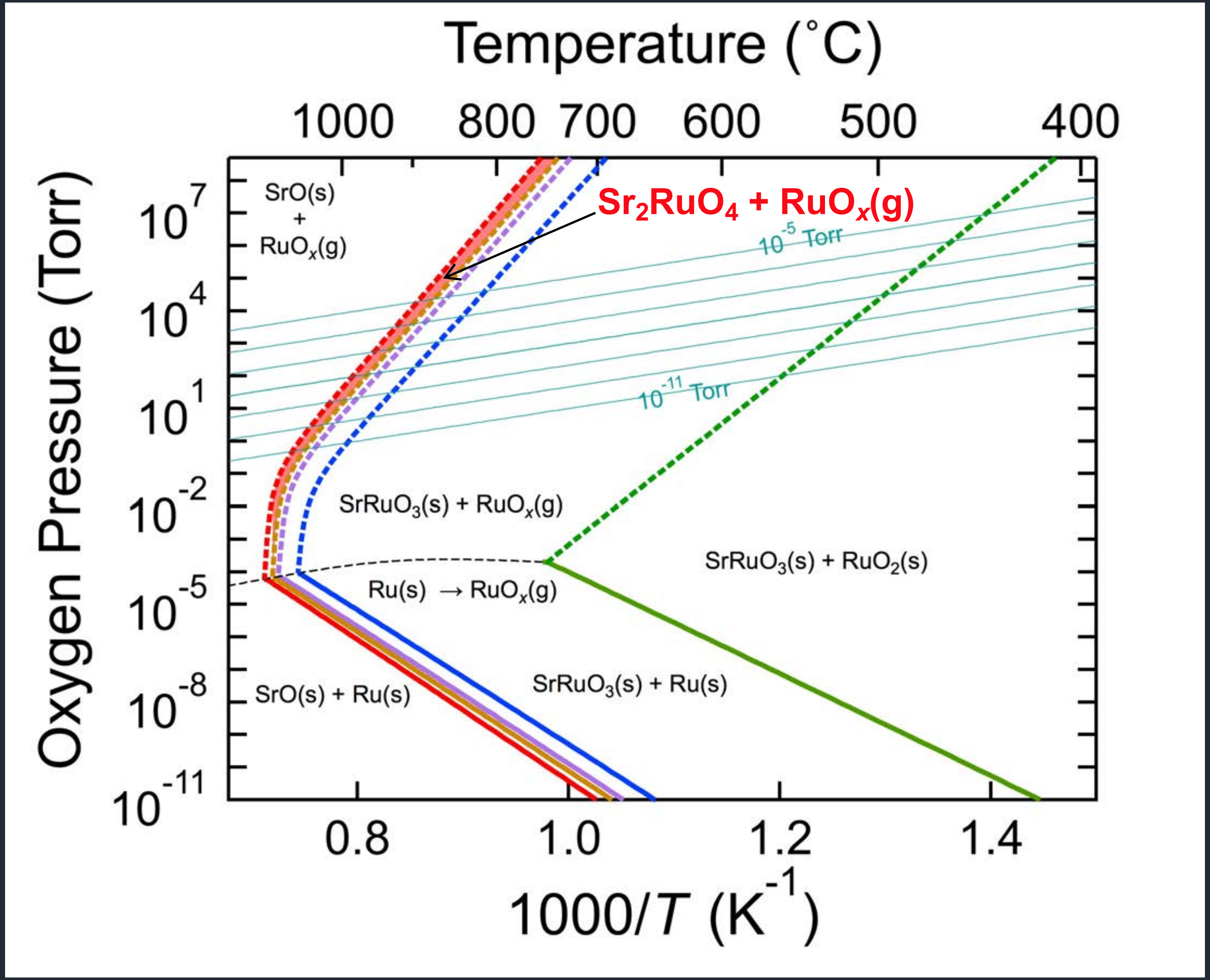

H.P. Nair, Y. Liu, J.P. Ruf, N.J. Schreiber, S-L. Shang, D.J. Baek, B.H. Goodge,
L.F. Kourkoutis, Z.K. Liu, K.M. Shen, and D.G. Schlom,
APL Materials **6** (2018) 046101.

Thermodynamics of $Sr_{n+1}Ru_nO_{3n+1}$ by MBE

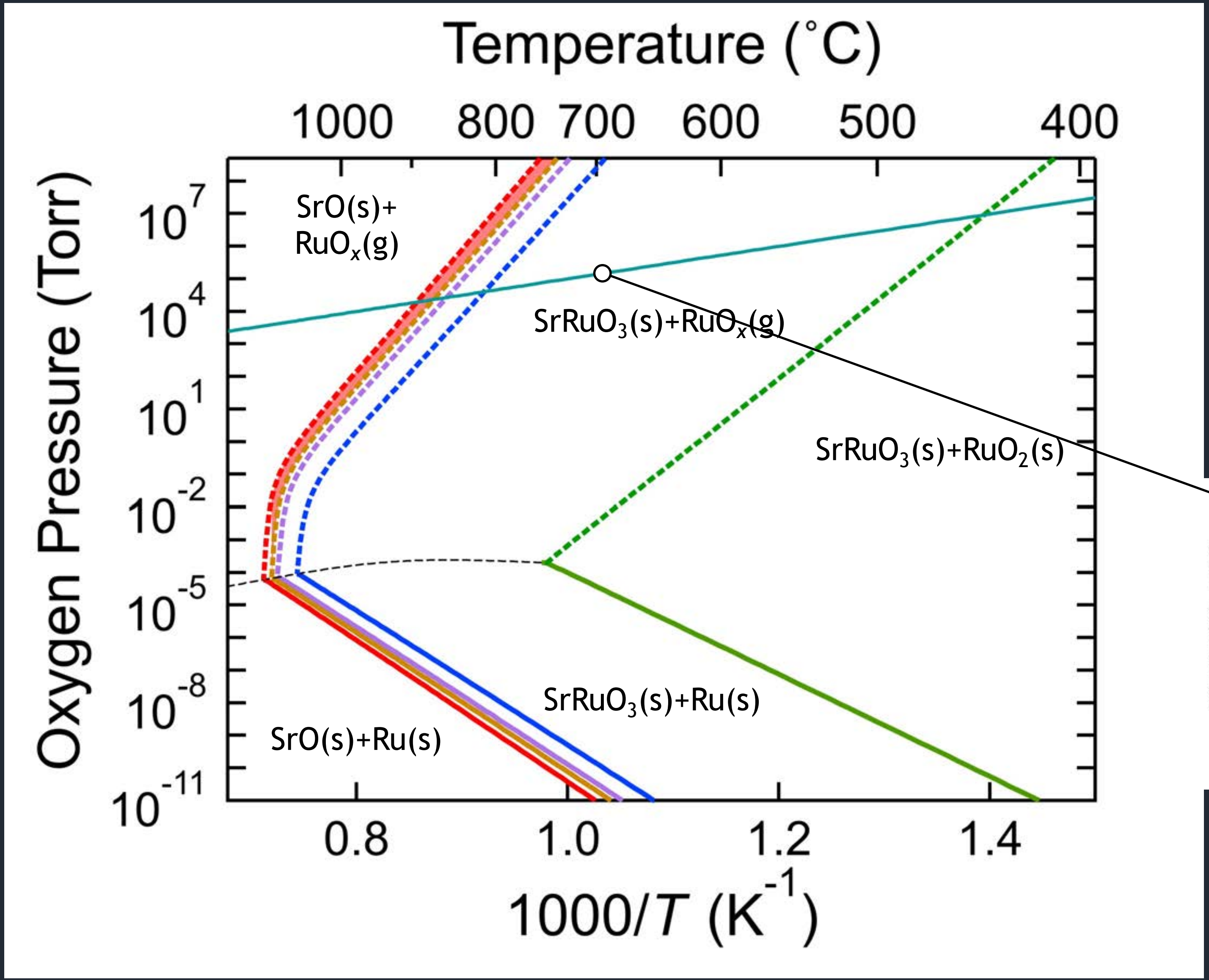

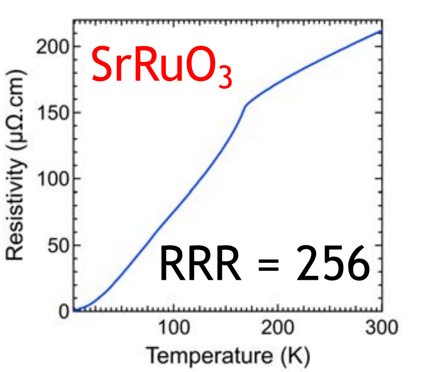

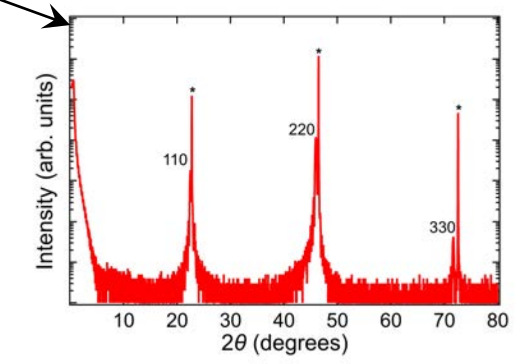

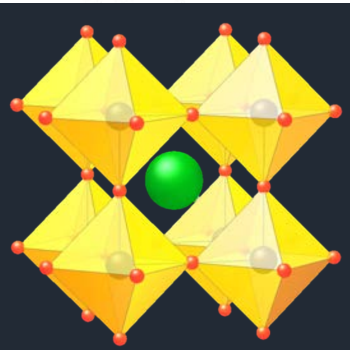

H.P. Nair, Y. Liu, J.P. Ruf, N.J. Schreiber, S-L. Shang, D.J. Baek, B.H. Goodge,
L.F. Kourkoutis, Z.K. Liu, K.M. Shen, and D.G. Schlom,
APL Materials **6** (2018) 046101.

Benchmarking $SrRuO_3$ Films and Crystals

Best PLD Film

$\rho_{300\,K} / \rho_{10\,K} = 14.1$

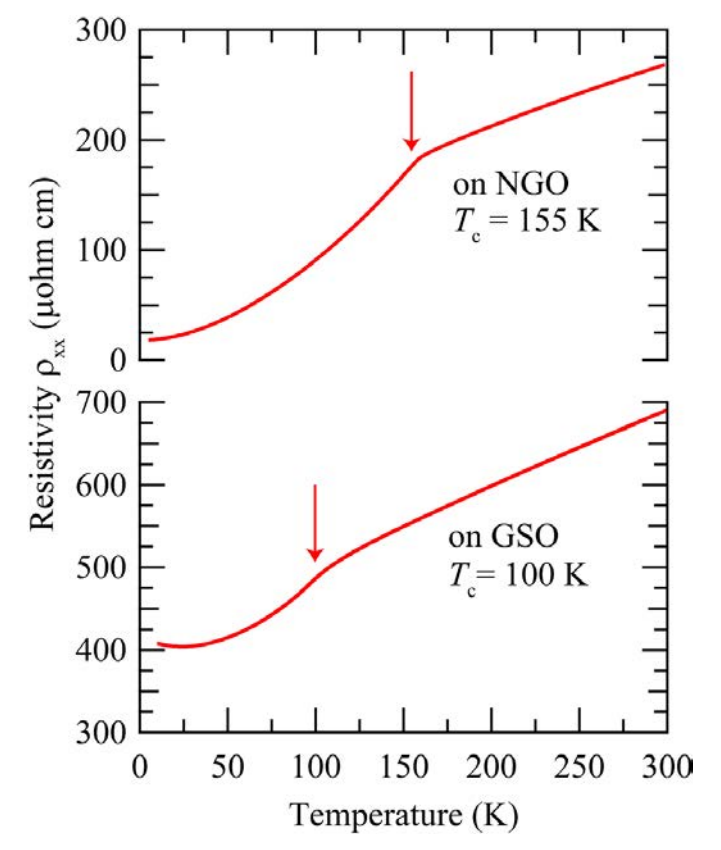

~20 nm $SrRuO_3$ / (110) $NdGaO_3$

D. Kan, R. Aso, H. Kurata, and Y. Shimakawa, *J. Appl. Phys.* **113** (2013) 173912 .

Best Prior MBE Film

$\rho_{300\,K} / \rho_{0\,K} = 60$

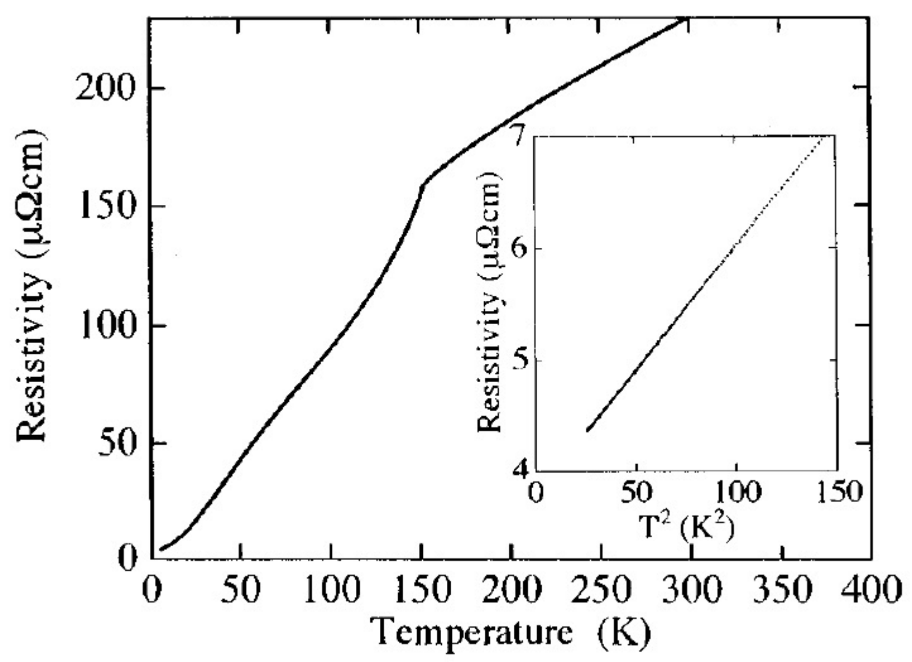

~100 nm $SrRuO_3$ / 2° miscut (100) $SrTiO_3$

A.P. MacKenzie, J.W. Reiner, A.W. Tyler, L.M. Galvin, S.R. Julian, M.R. Beasley, T.H. Geballe, and A. Kapitulnik, *Physical Review B* **58** (1998) 13318–13321.

Best Single Crystal

$\rho_{300\,K} / \rho_{0\,K} = 192$

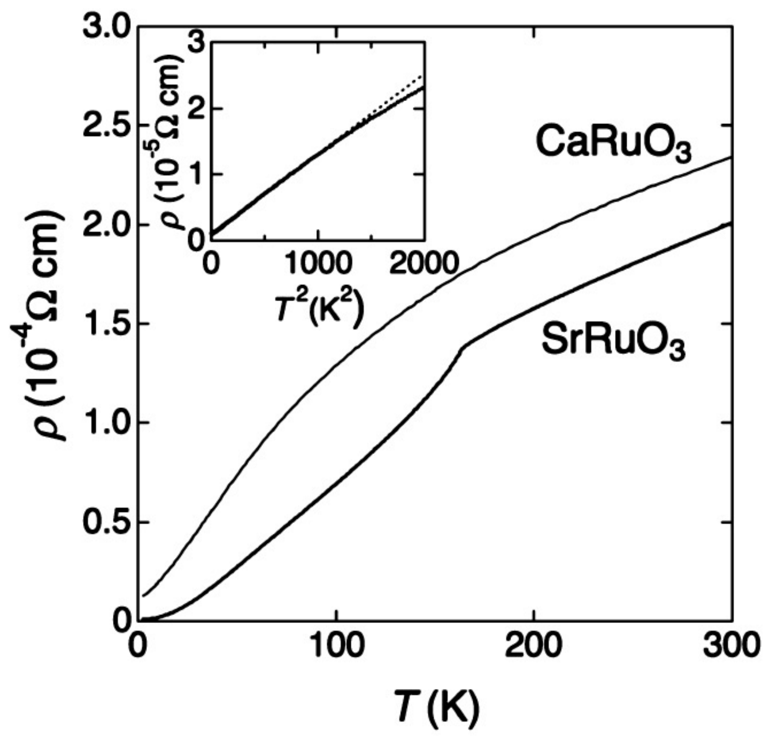

$SrRuO_3$ single crystal

N. Kikugawa, R. Baumbach, J.S. Brooks, T. Terashima, S. Uji, and Y. Maeno, *Crystal Growth & Design* **15** (2015) 5573–5577.

Thermodynamics of $Sr_{n+1}Ru_nO_{3n+1}$ by MBE

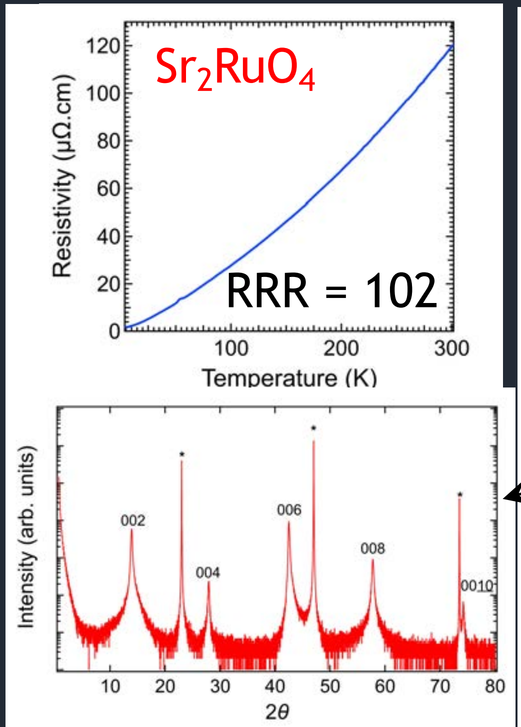

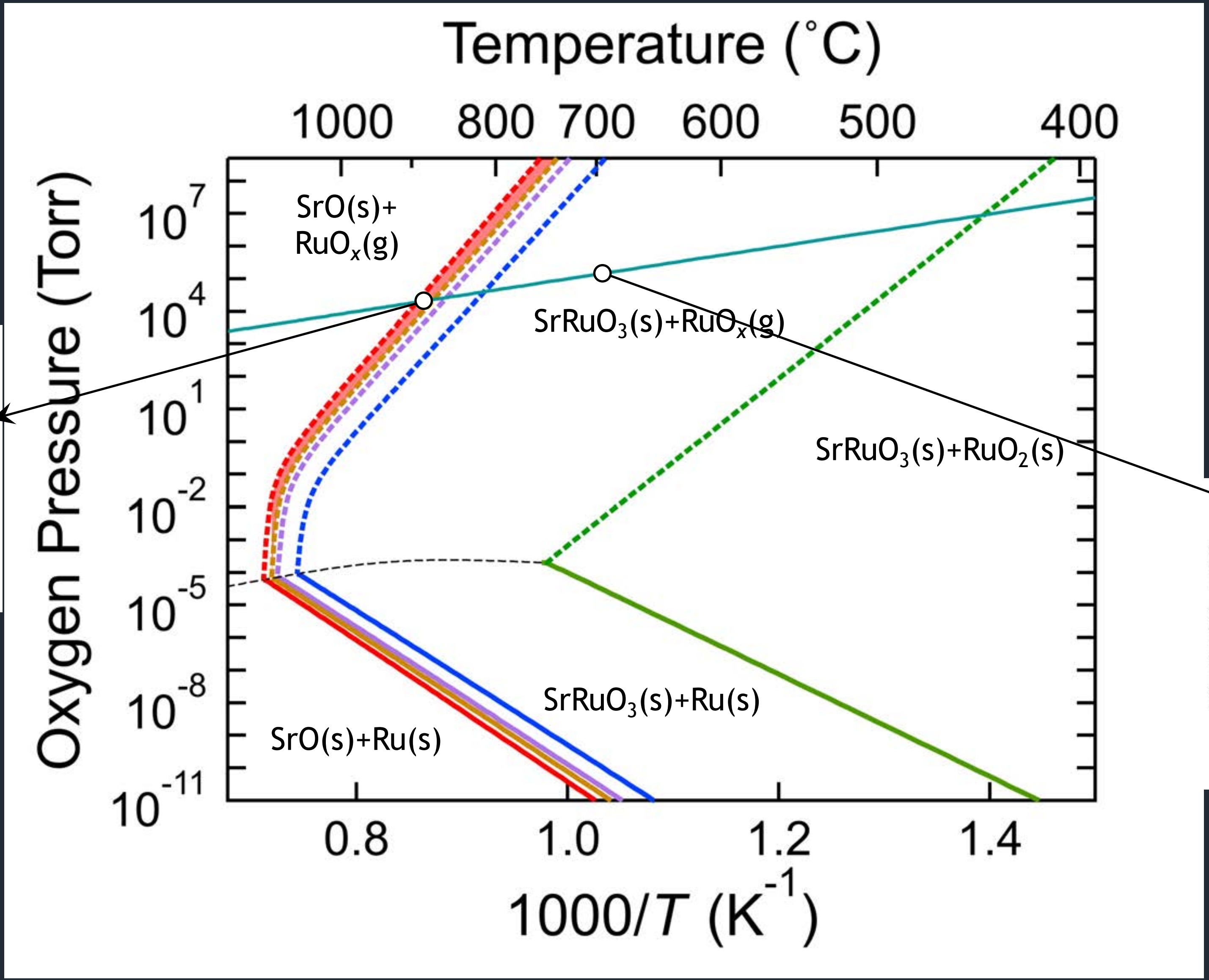

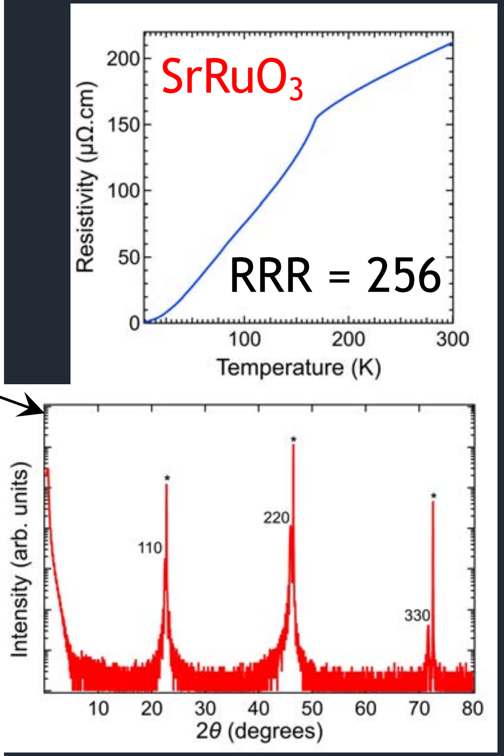

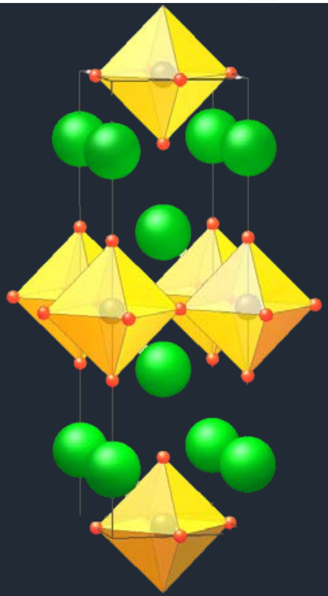

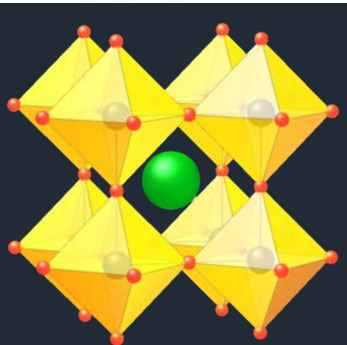

H.P. Nair, Y. Liu, J.P. Ruf, N.J. Schreiber, S-L. Shang, D.J. Baek, B.H. Goodge,
L.F. Kourkoutis, Z.K. Liu, K.M. Shen, and D.G. Schlom,
APL Materials **6** (2018) 046101.

Superconducting Sr_2RuO_4 Films

55 nm thick Sr_2RuO_4 on (110) $NdGaO_3$

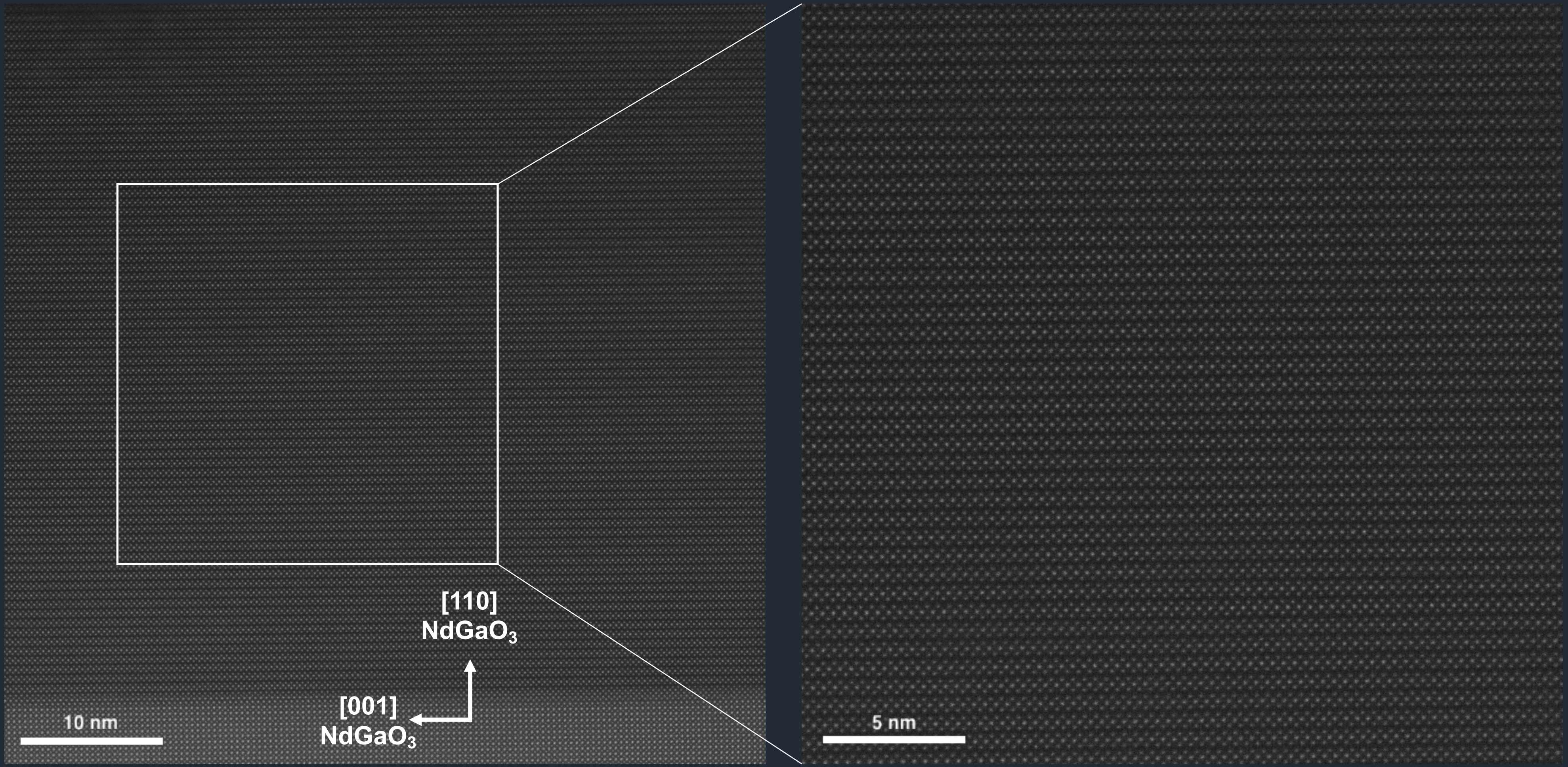


Berit Goodge

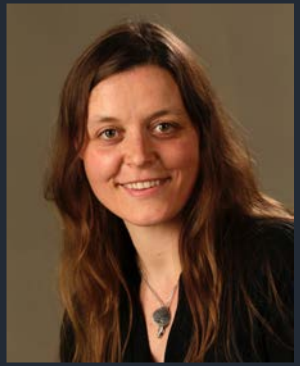
Lena Kourkoutis

Challenge

What if the oxide you desire cannot be grown by adsorption-control?

$Sr_7Ti_6O_{19}$

$BaSr_6Ti_6O_{19}$

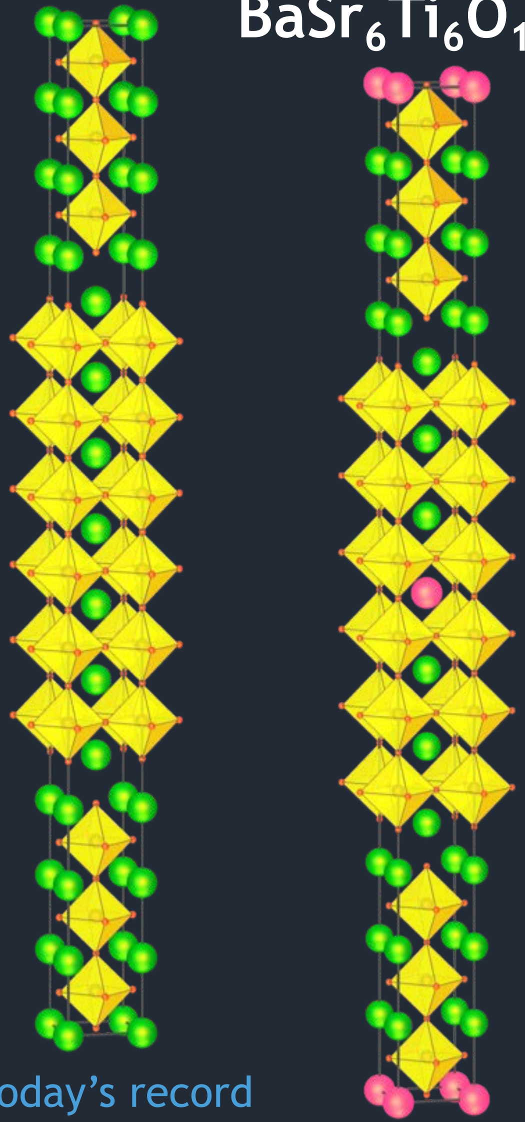

today's record tunable microwave dielectric

Composition Control

- Adsorption-Controlled Growth
- Flux-Controlled Growth

RHEED and RHEED Oscillations

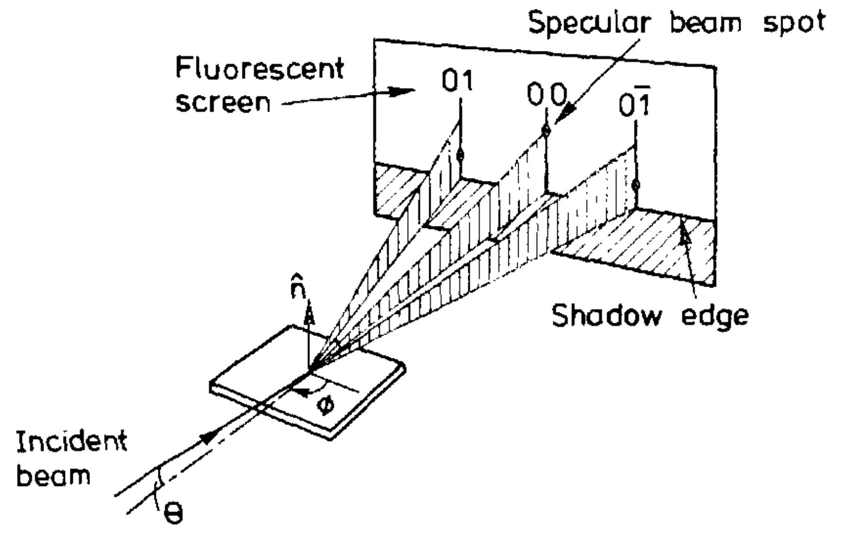

FIG. 1. Schematic diagram of RHEED geometry showing the incident beam at an angle θ to the surface plane; azimuthal angle φ. The elongated spots indicate the intersection of the Ewald sphere with the 01, 00, and 0$\bar{1}$ rods.

B. Bölger and P. K. Larsen
Review of Scientific Instruments **57** (1986) 1363-1367.

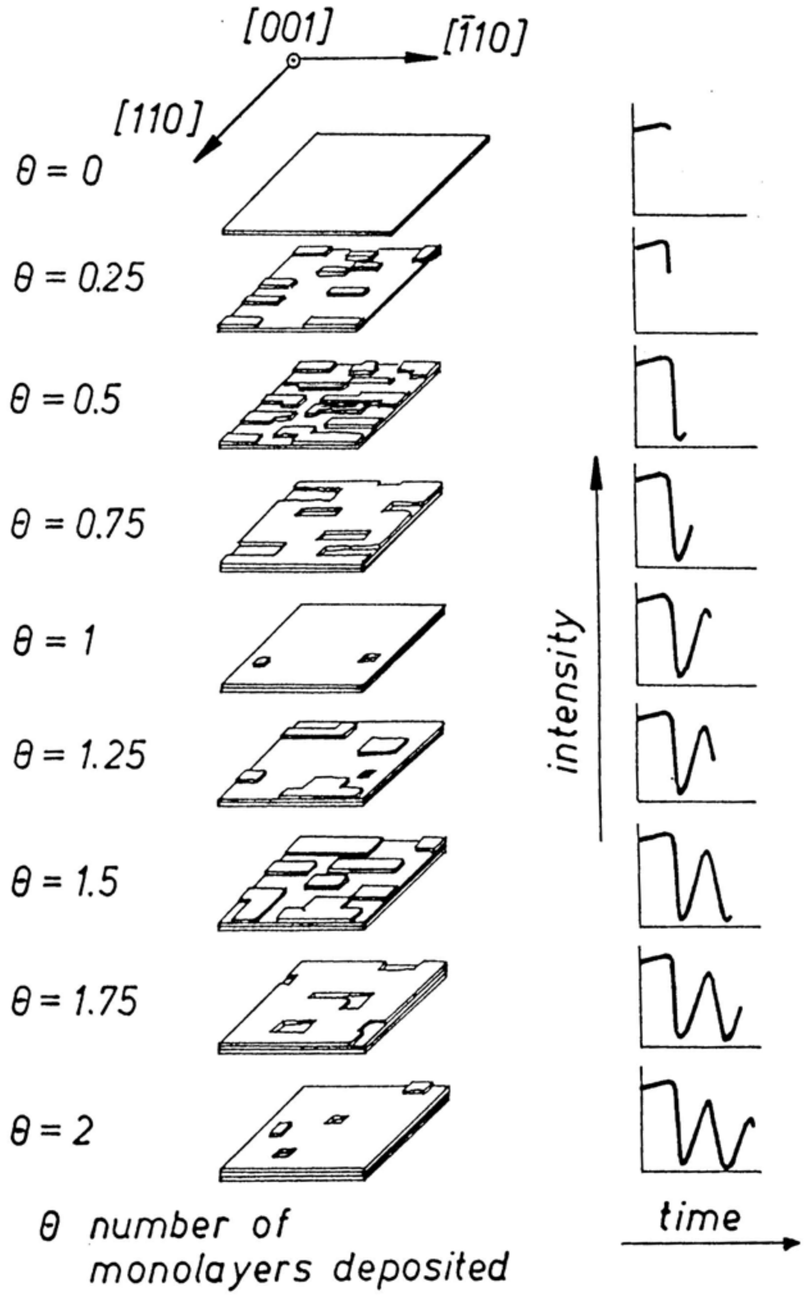

B.A. Joyce, P.J. Dobson, J.H. Neave, K. Woodbridge,
J. Zhang, P.K. Larsen, and B Bölger,
Surface Science **168** (1986) 423-438.

RHEED Oscillations

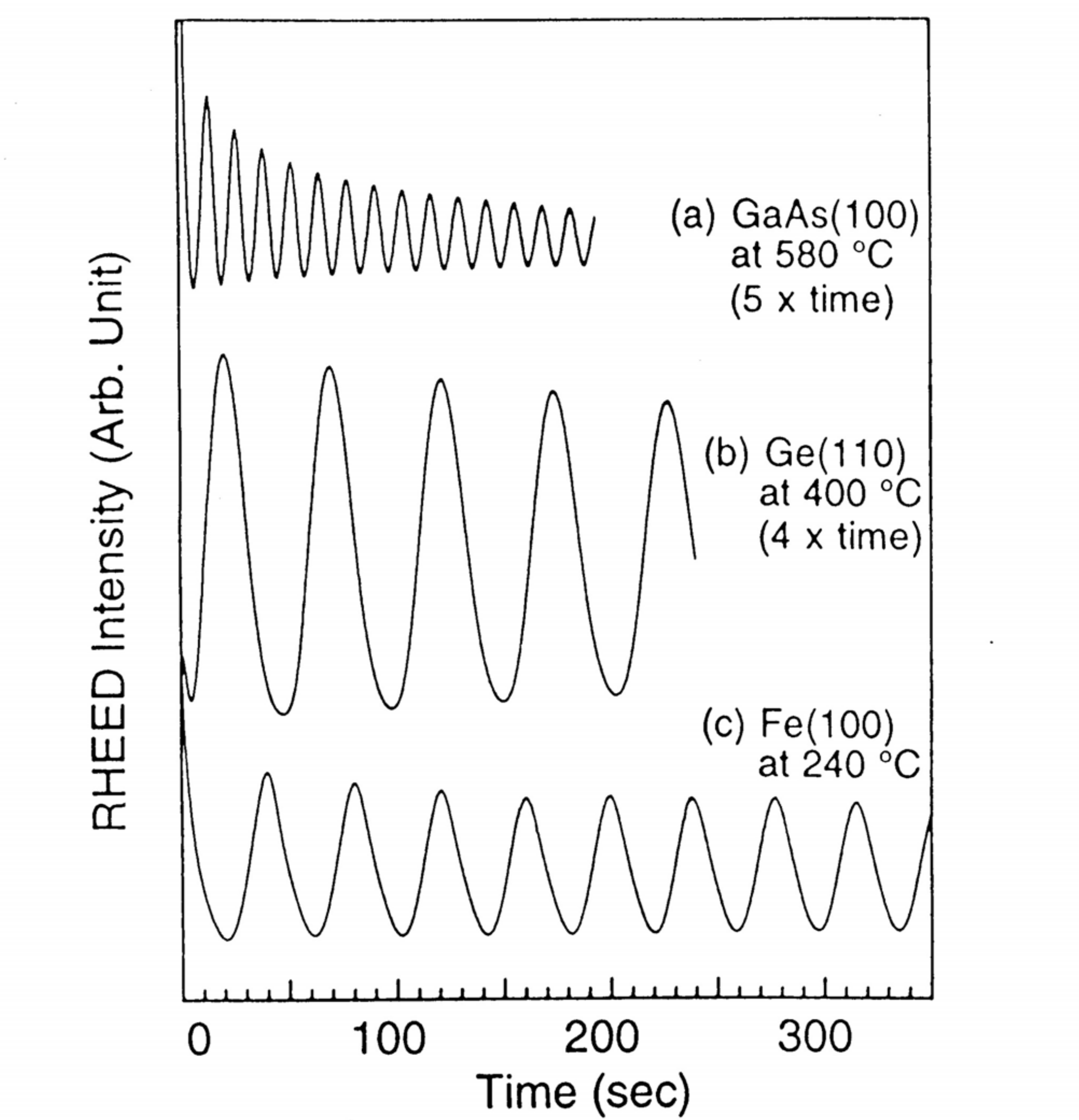

Molecular Beam Epitaxy: Applications to Key Materials
edited by R.F.C. Farrow (Noyes, Park Ridge, 1995), p. 694.

RHEED Oscillations

$BaTiO_3$

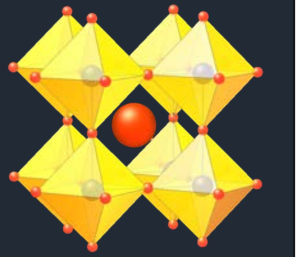

La_2CuO_4

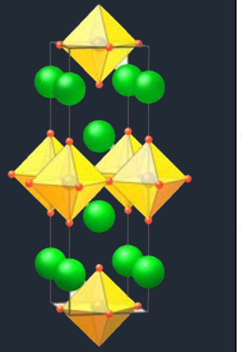

$YBa_2Cu_3O_7$

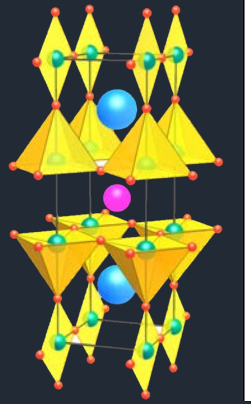

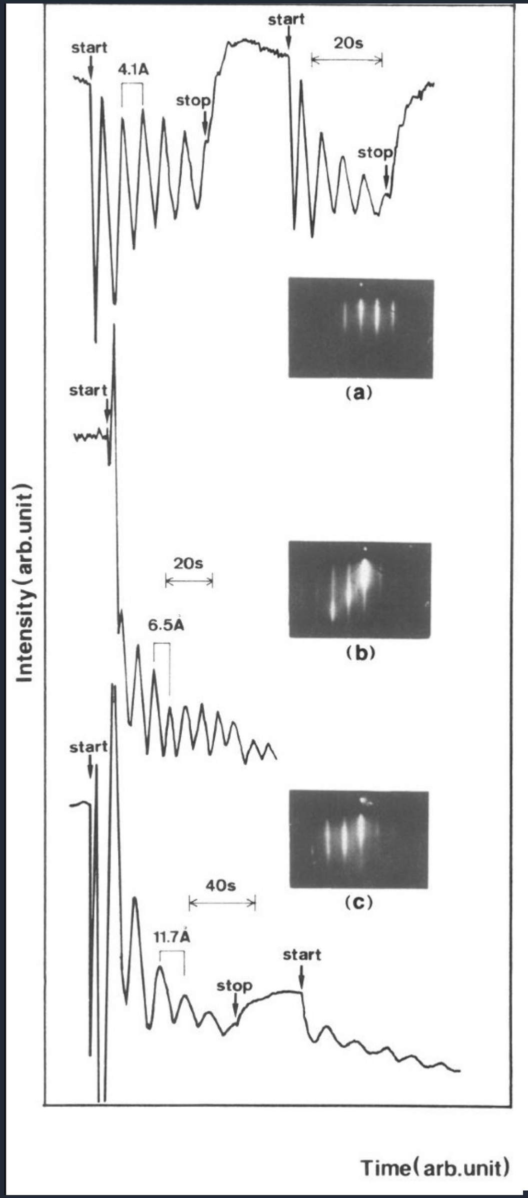

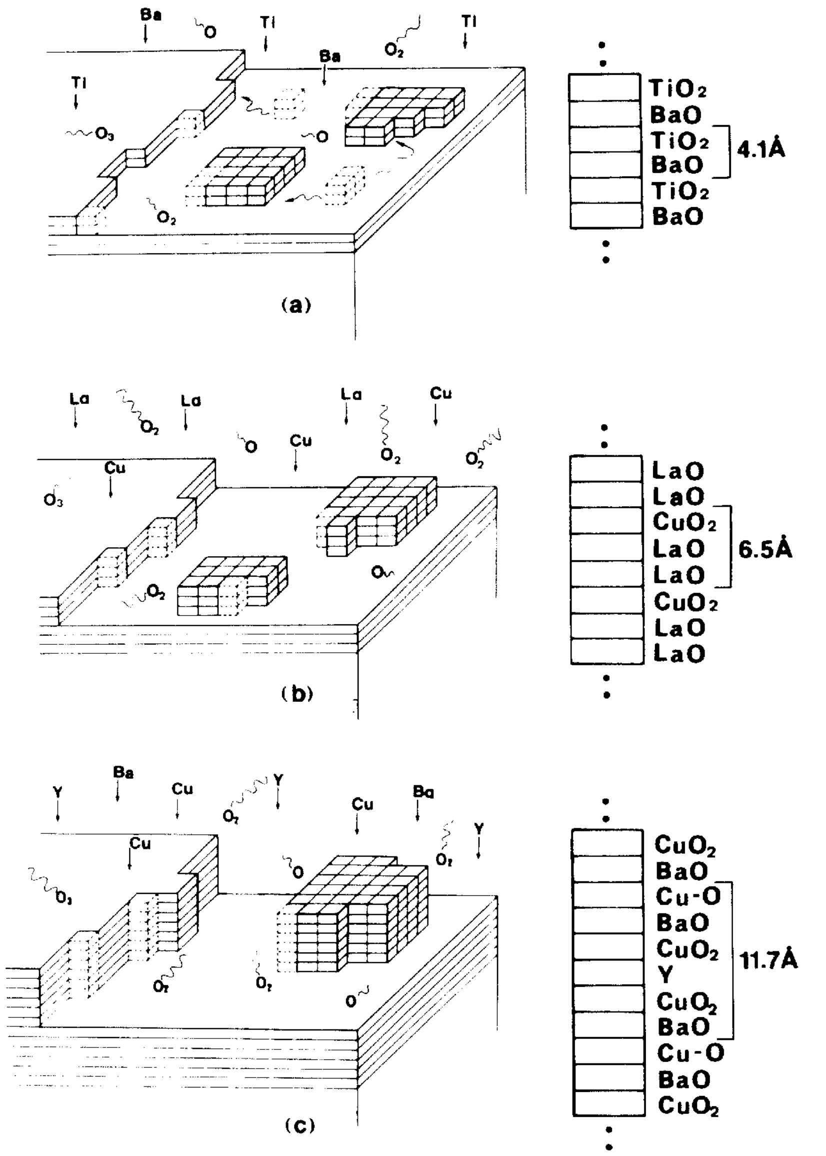

T. Terashima, Y. Bando, K. Iijima, K. Yamamoto, K. Hirata, K. Hayashi, K. Kamigaki, and H. Terauchi, *Physical Review Letters* **65** (1990) 2684-2687.

How to Calibrate Growth Rate

- Shadow Mask and Surface Profilometer
- Quartz Crystal Microbalance
- Ion Gauge
- RHEED Oscillations (and shuttered RHEED oscillations)
- Changes in RHEED Pattern (e.g., reconstructions)
- Rutherford Backscattering Spectrometry
- Mass Spectrometer
- Atomic Absorption Spectroscopy
- Atomic Emission Spectroscopy
- X-Ray Reflectivity
- Ellipsometry, …

Binary Oxide Calibration Method

- RHEED Oscillations or X-Ray Reflectivity

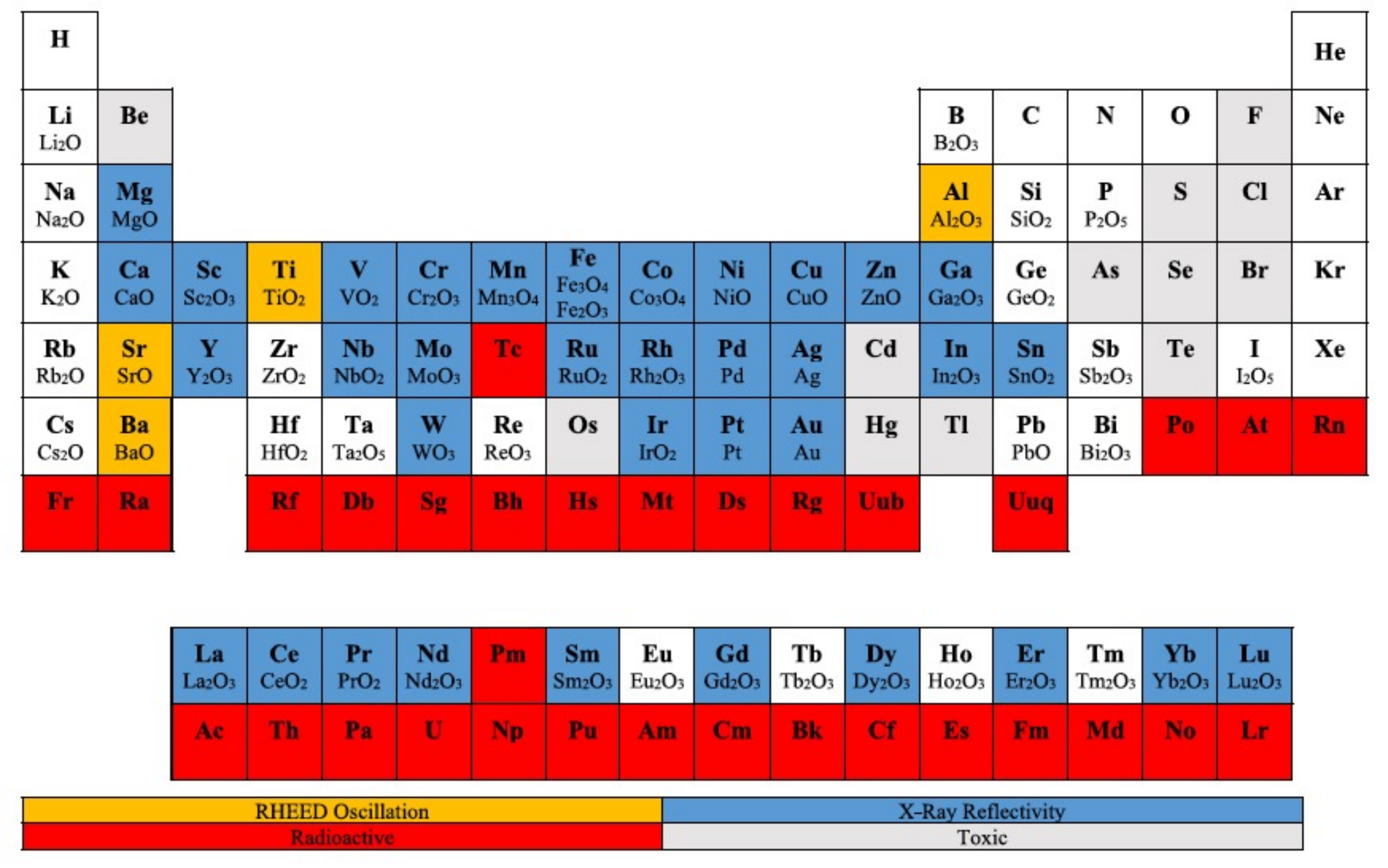

H																	**He**
Li Li_2O	▨ **Be**											**B** B_2O_3	**C**	**N**	**O**	▨ **F**	**Ne**
Na Na_2O	🟦 **Mg** MgO											🟧 **Al** Al_2O_3	**Si** SiO_2	**P** P_2O_5	▨ **S**	▨ **Cl**	**Ar**
K K_2O	🟦 **Ca** CaO	🟦 **Sc** Sc_2O_3	🟧 **Ti** TiO_2	🟦 **V** VO_2	🟦 **Cr** Cr_2O_3	🟦 **Mn** Mn_3O_4	🟦 **Fe** Fe_3O_4 Fe_2O_3	🟦 **Co** Co_3O_4	🟦 **Ni** NiO	🟦 **Cu** CuO	🟦 **Zn** ZnO	🟦 **Ga** Ga_2O_3	**Ge** GeO_2	▨ **As**	▨ **Se**	▨ **Br**	**Kr**
Rb Rb_2O	🟧 **Sr** SrO	🟦 **Y** Y_2O_3	**Zr** ZrO_2	🟦 **Nb** NbO_2	🟦 **Mo** MoO_3	🟥 **Tc**	🟦 **Ru** RuO_2	🟦 **Rh** Rh_2O_3	🟦 **Pd** Pd	🟦 **Ag** Ag	▨ **Cd**	🟦 **In** In_2O_3	🟦 **Sn** SnO_2	**Sb** Sb_2O_3	▨ **Te**	**I** I_2O_5	**Xe**
Cs Cs_2O	🟧 **Ba** BaO		**Hf** HfO_2	**Ta** Ta_2O_5	🟦 **W** WO_3	**Re** ReO_3	▨ **Os**	🟦 **Ir** IrO_2	🟦 **Pt** Pt	🟦 **Au** Au	▨ **Hg**	▨ **Tl**	**Pb** PbO	**Bi** Bi_2O_3	🟥 **Po**	🟥 **At**	🟥 **Rn**
🟥 **Fr**	🟥 **Ra**		🟥 **Rf**	🟥 **Db**	🟥 **Sg**	🟥 **Bh**	🟥 **Hs**	🟥 **Mt**	🟥 **Ds**	🟥 **Rg**	🟥 **Uub**		🟥 **Uuq**				
		🟦 **La** La_2O_3	🟦 **Ce** CeO_2	🟦 **Pr** PrO_2	🟦 **Nd** Nd_2O_3	🟥 **Pm**	🟦 **Sm** Sm_2O_3	**Eu** Eu_2O_3	🟦 **Gd** Gd_2O_3	**Tb** Tb_2O_3	🟦 **Dy** Dy_2O_3	**Ho** Ho_2O_3	🟦 **Er** Er_2O_3	**Tm** Tm_2O_3	🟦 **Yb** Yb_2O_3	🟦 **Lu** Lu_2O_3	
		🟥 **Ac**	🟥 **Th**	🟥 **Pa**	🟥 **U**	🟥 **Np**	🟥 **Pu**	🟥 **Am**	🟥 **Cm**	🟥 **Bk**	🟥 **Cf**	🟥 **Es**	🟥 **Fm**	🟥 **Md**	🟥 **No**	🟥 **Lr**	

🟧 RHEED Oscillation	🟦 X-Ray Reflectivity
🟥 Radioactive	▨ Toxic

J. Sun, C.T. Parzyck,
J.H. Lee, C.M. Brooks,
L.F. Kourkoutis, X. Ke,
R. Misra, J. Schubert,
F.V. Hensling, M.R. Barone,
Z. Wang, M.E. Holtz,
N.J. Schreiber, Q. Song, H. Paik,
T. Heeg, D.A. Muller,
K.M. Shen, and D.G. Schlom,
Physical Review Materials **6**
(2022) 033802.

Binary Oxide Calibration Method

Example: Calibration to grow $La_{1/2}Sr_{1/2}CoO_3$

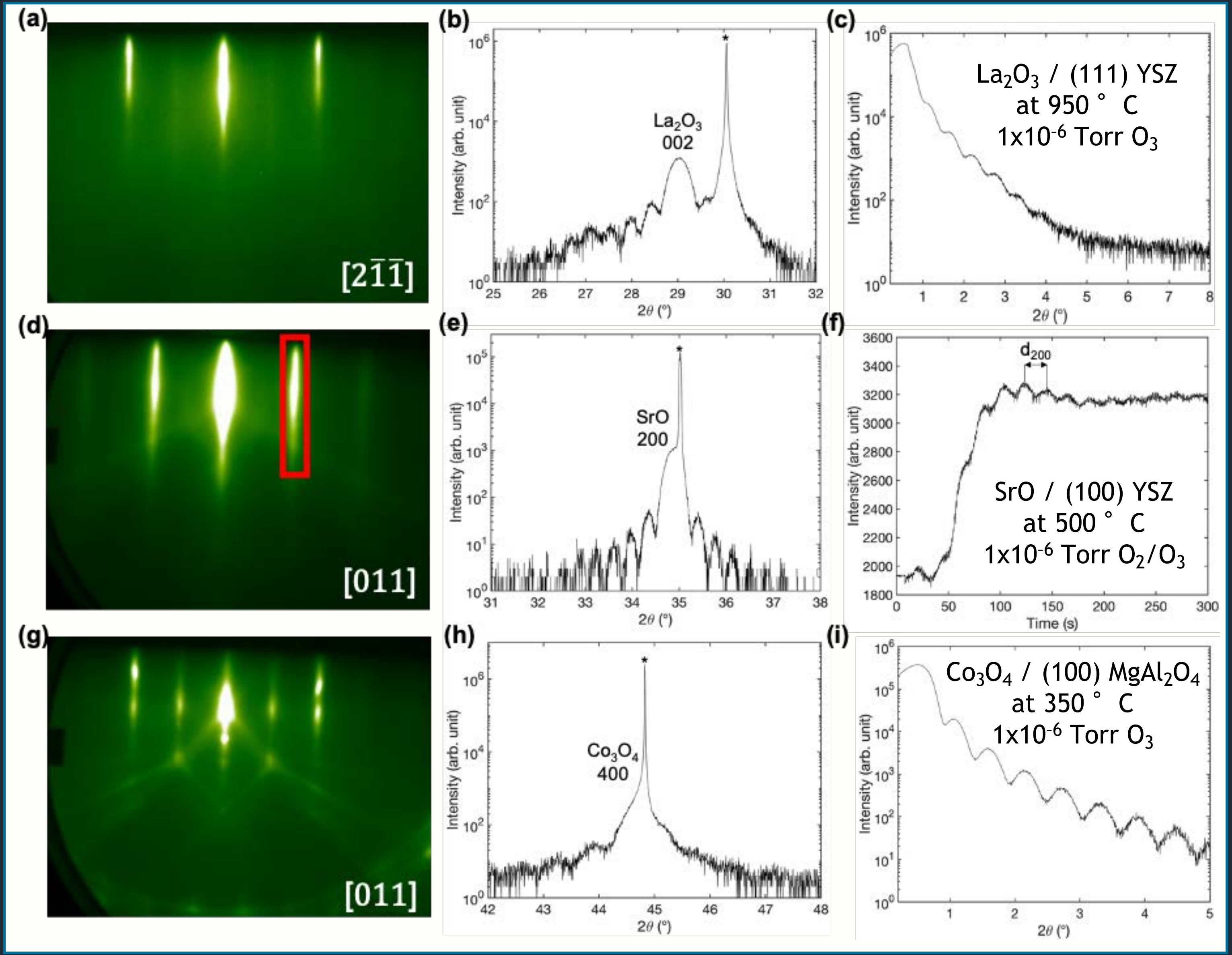

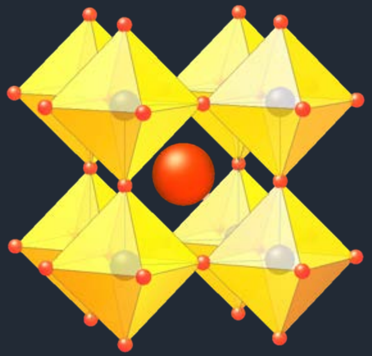

J. Sun, C.T. Parzyck,
J.H. Lee, C.M. Brooks,
L.F. Kourkoutis, X. Ke,
R. Misra, J. Schubert,
F.V. Hensling, M.R. Barone,
Z. Wang, M.E. Holtz,
N.J. Schreiber, Q. Song, H. Paik,
T. Heeg, D.A. Muller,
K.M. Shen, and D.G. Schlom,
Physical Review Materials **6**
(2022) 033802.

Today's Highest-*n* Ruddlesden-Popper

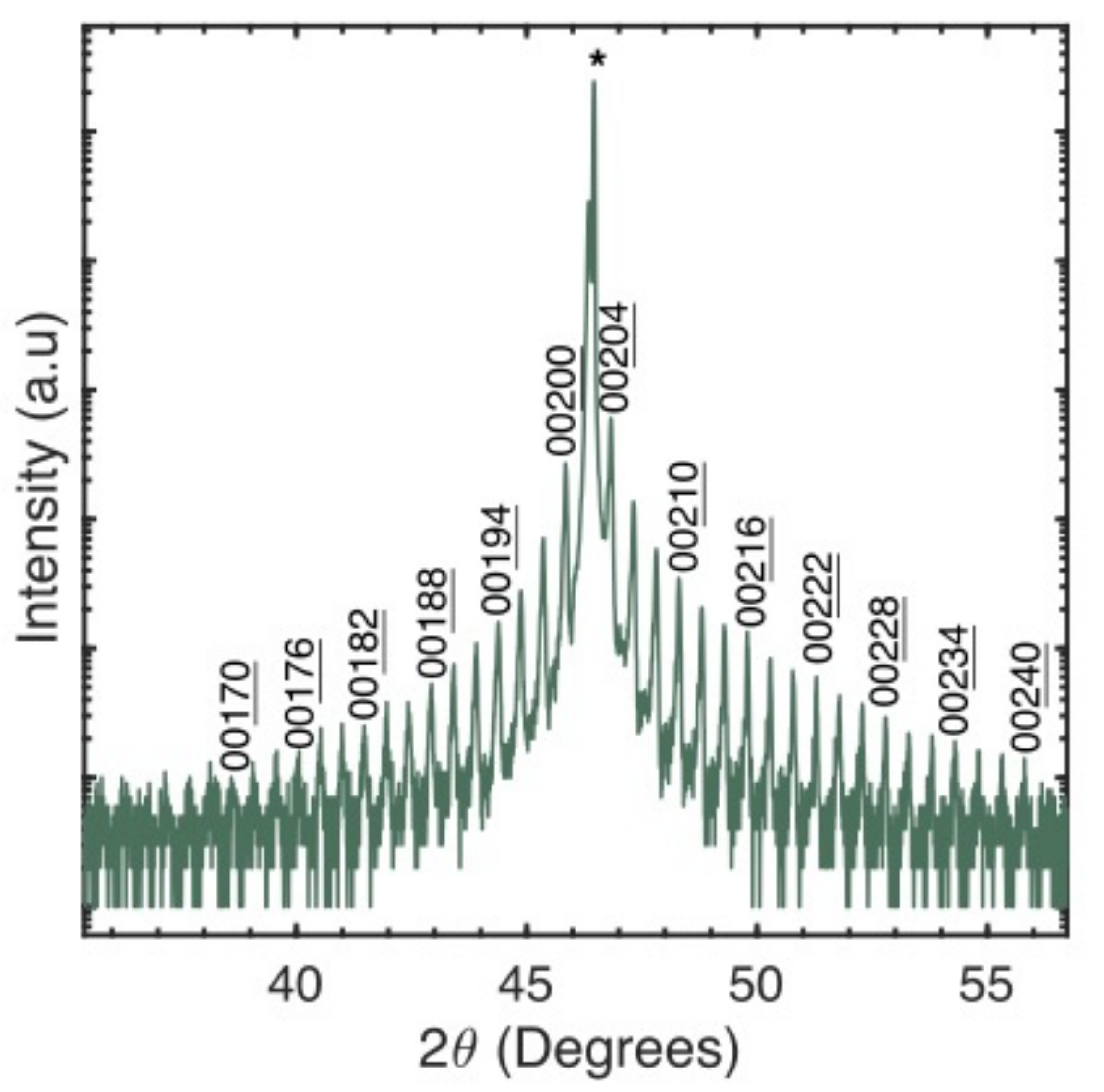

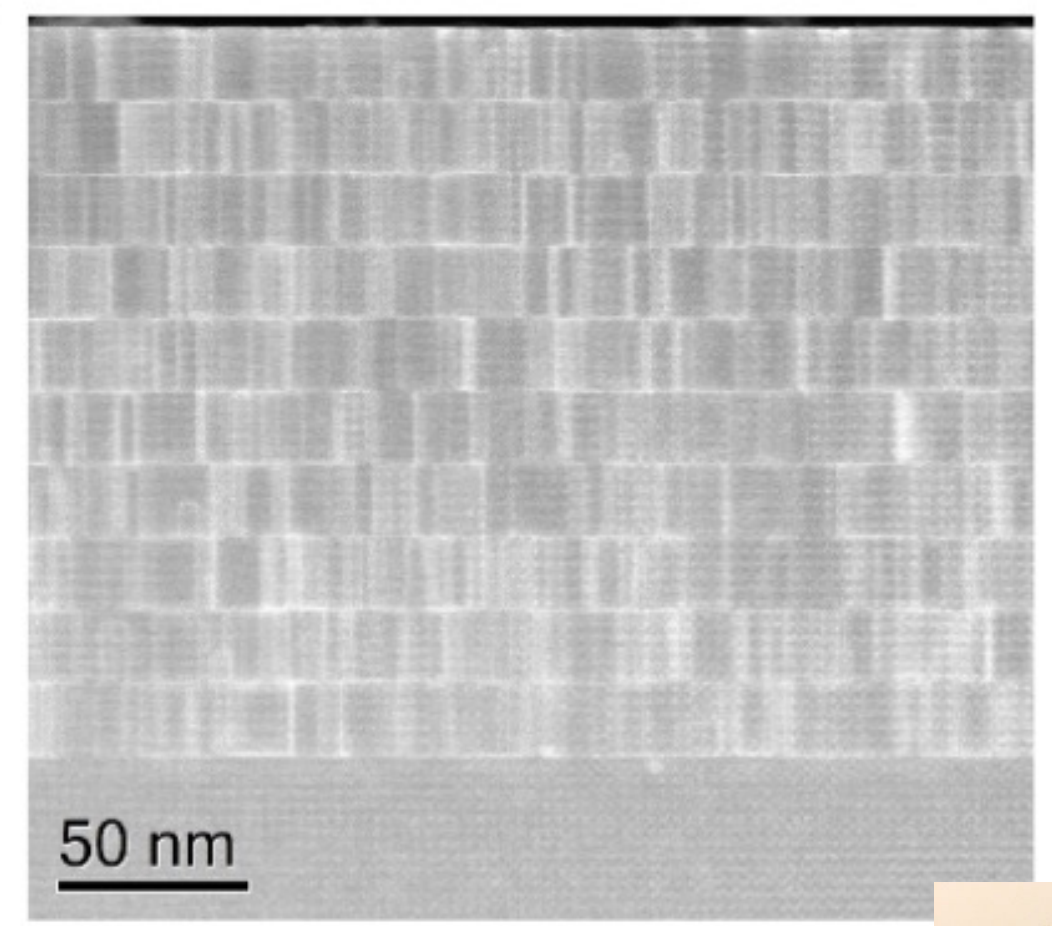

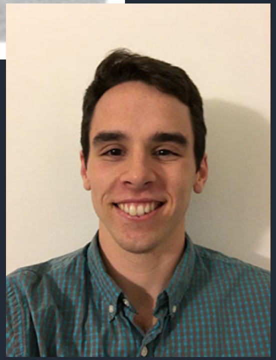

Matt Barone

Calibration by RHEED Reconstruction

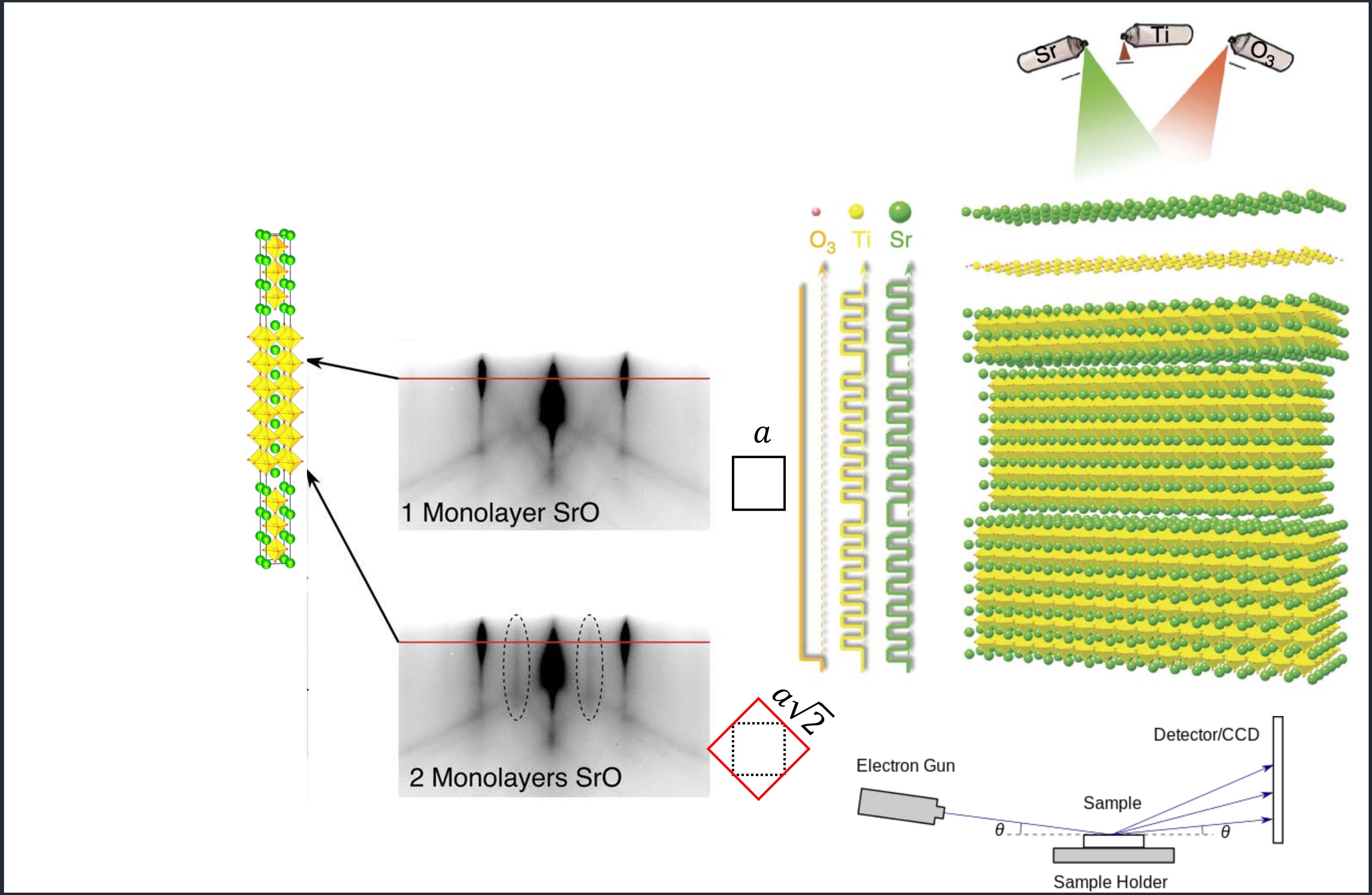

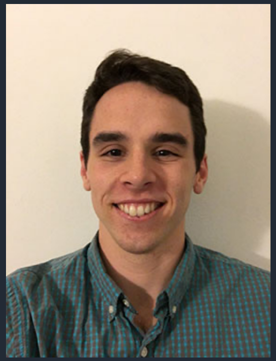

Matt Barone

Calibration by RHEED Reconstruction

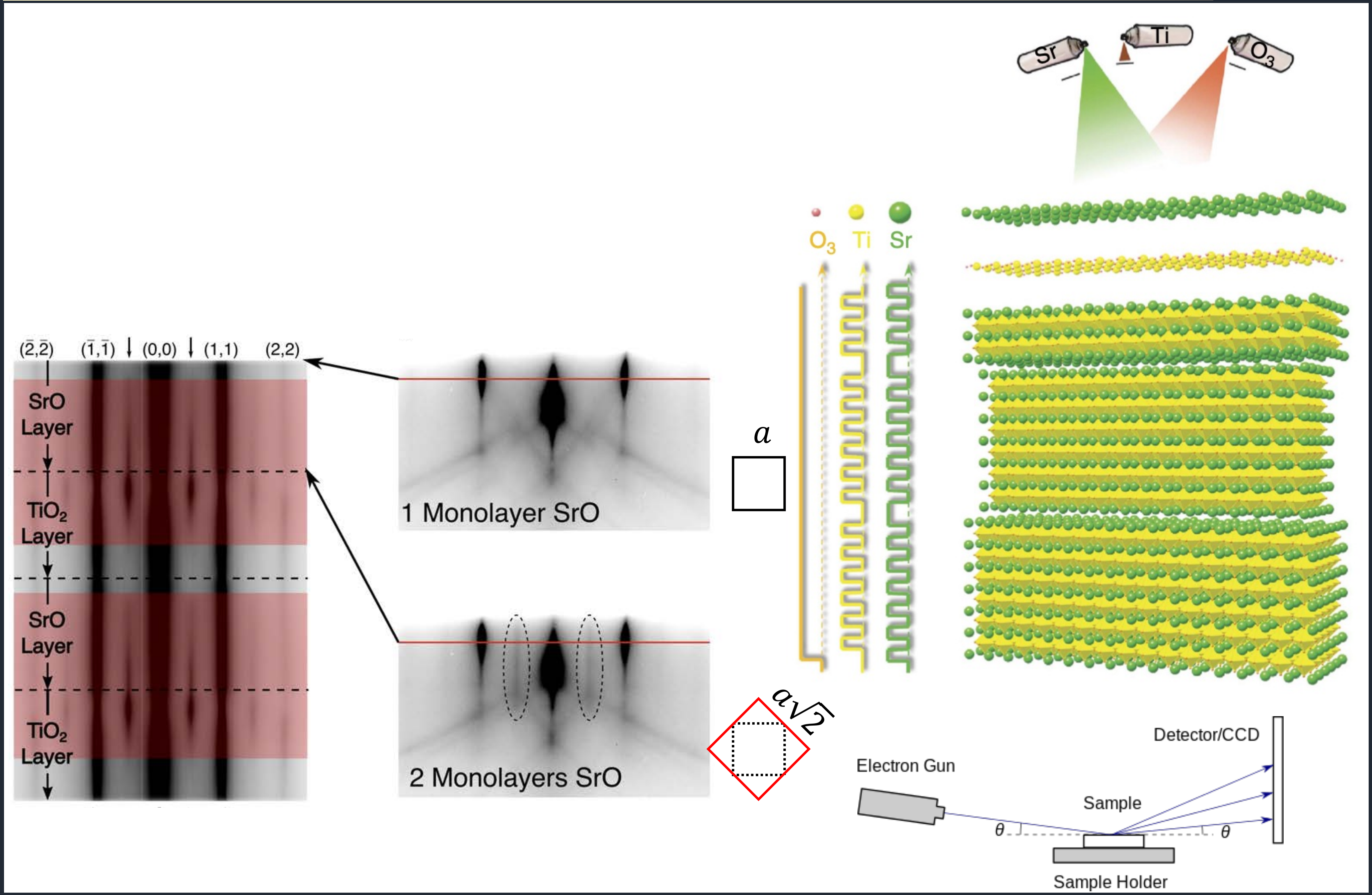

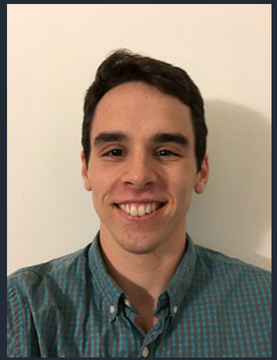

Matt Barone

Calibration by RHEED Reconstruction

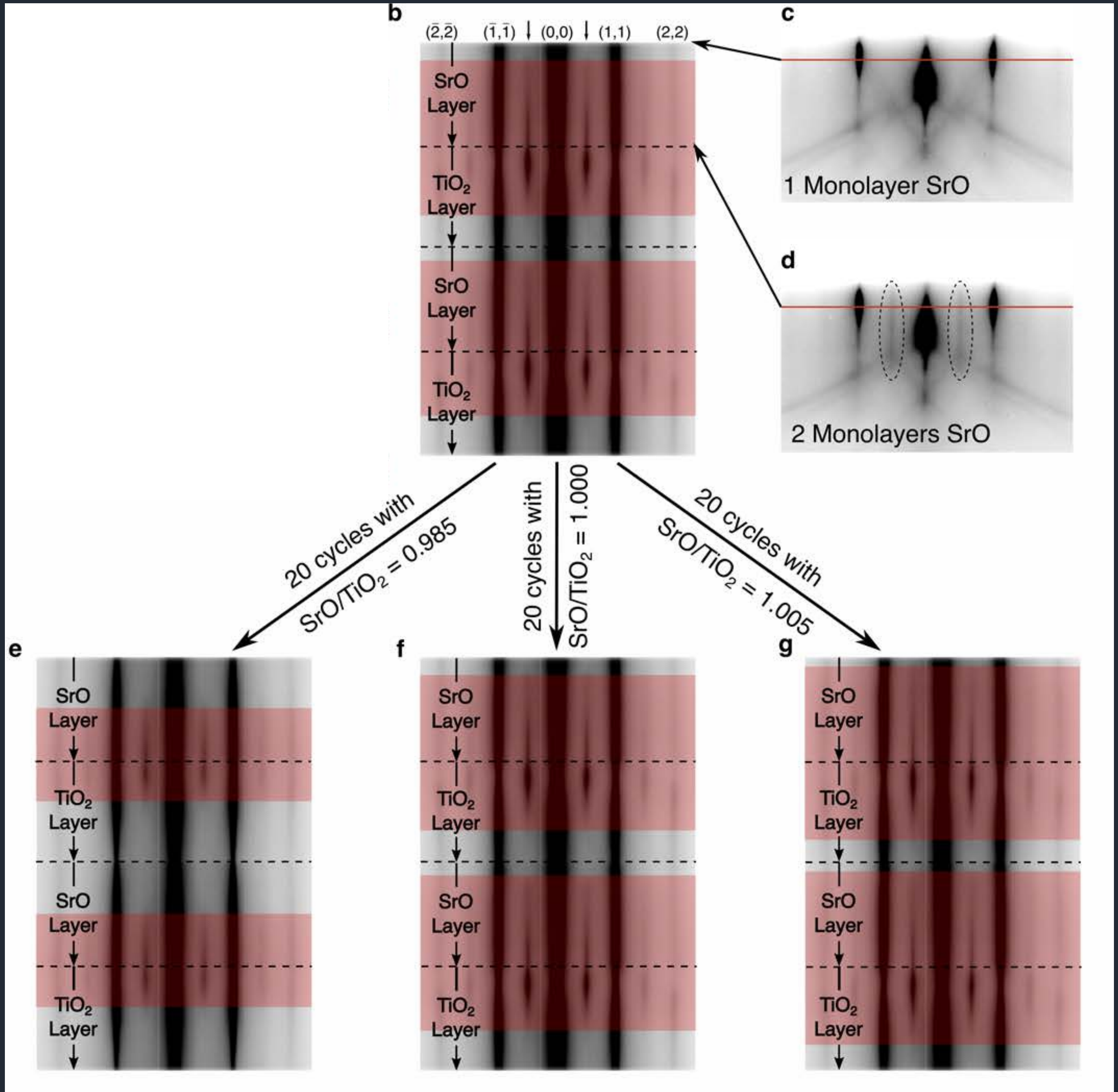

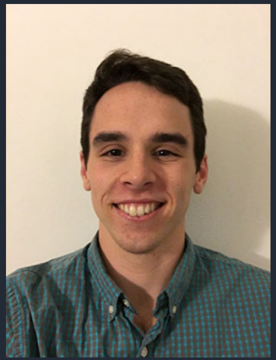

Matt Barone